Accepted Manuscript

Journal of the Geological Society

3D Seismic classification of Fluid Escape Pipes in the western Exmouth Plateau, North West Shelf of Australia (A)

Susy Mercado Ruge, Nicola Scarselli & Awad Bilal

DOI: https://doi.org/10.1144/jgs2020-096

To access the most recent version of this article, please click the DOI URL in the line above.

Received 29 May 2020
Revised 29 October 2020
Accepted 30 October 2020

3D Seismic classification of Fluid Escape Pipes in the western Exmouth Plateau, North West Shelf of Australia (A)

Susy Mercado Ruge [a,*] *Nicola Scarselli* [a,] *and Awad Bilal* [a,b]

[a] Department of Earth Sciences, Royal Holloway University of London, Egham, Surrey TW20 0EX, UK

[b] *Department of Earth Sciences, Faculty of Science, University of Benghazi, PO. Box 9480, Benghazi, Libya*

Correspondence: susymercadoruge@gmail.com

Keywords: fluid escape pipes, fluid flow, pockmarks, extensional faults, overpressure, North West Shelf, Australia

Abstract (B)

Fluid escape pipes are vertical pathways of focused flow venting from a variety of deep overpressure sources. These geological features are typical of many sedimentary basins, including proven petroliferous provinces worldwide, such as the North Sea and the Exmouth Plateau in the Northern Carnarvon Basin, Northwest Australia. High quality three-dimensional (3D) seismic reflection data from the western Exmouth Plateau revealed the occurrence of exceptionally well-imaged fluid escape pipes affecting the Jurassic strata and the Triassic Mungaroo Formation, a key reservoir unit in the basin. A total of 171 fluid escape pipes, including blowout, seepage and hydrothermal pipes, were mapped, and their geomorphic characteristics were analysed. In the study area, these features form prominent vertical columns up to 4.5 km long disrupting continuous reflections of the Triassic to Jurassic section. Numerous fluid escape pipes terminate with paleo-pockmarks affecting at the Upper Jurassic syn-extension strata, providing evidence for pipe genesis during the early stages of the Late Jurassic rifting in the Exmouth Plateau . Fluid escape pipes were found rooting from different stratigraphic levels, suggesting multiple fluid sources within the Triassic sediments. Several fluid flow structures nucleated along or nearby rift-related fault planes within

the Mungaroo Formation providing further evidence of rifting as a main triggering factor of important fluid flow in the basin.

In the study area, the presence of fluid escape pipes represents a significant risk for the preservation of potential hydrocarbons accumulations as when these features form, vertical fluid venting breaches through stratigraphy compromising the integrity of seal units. This seems supported by the lack of significant discoveries within the area covered by seismic survey analysed in this research.

Introduction (B)

Fluid escape pipes are key geological features that control fluid flow, including hydrocarbon migration, in sedimentary basins (Ligtenberg, 2005; Cartwright *et al*. 2007; Cartwright and Santamaria, 2015). These have been documented in many rift and passive margin settings such as the North Sea (Underhill, 2009), the Karoo Basin of South Africa (Svensen *et al.* 2006), offshore Nigeria (Haskell *et al.* 1999), in the Congo Basin (Gay *et al.* 2003), along the Norwegian margin (Svensen *et al.* 2004) and in the Exmouth Plateau (Velayatham *et al.* 2018; 2019).

These structures result from vertical and sub-vertical uplift of focused fluid flow (e.g. oil, gas, groundwater and magmatic fluids) venting from a source at depth to the seabed or land surface (Løseth *et al.* 2009, Andresen, 2012). Seismically, fluid escape pipes are defined by columnar zones of highly discontinuous reflections that terminate in erosive, circular depressions referred as to paleo-pockmarks, which are commonly associated with amplitude and velocity anomalies (Moss and Cartwright 2010; Cartwright and Santamaria, 2015; Velayatham *et al*. 2018; 2019; Omosanya *et al.* 2020; Foschi and Cartwright 2020).

In rift basins, fluid flow is commonly influenced by extensional faults that may act as conduits or barriers for fluid flow, depending on their three-dimensional geometry and growth history (Cartwright *et al*. 2007; Magee *et al.* 2015; Roelofse *et al.* 2020). Subsurface interactions between extensional faults and fluids may thus affect fluid migration pathways and distributions (Magee *et al.* 2015).

In the Exmouth Plateau, fluid escape pipes appear to significantly affect the Triassic Mungaroo Formation (Fig. 1a), the main reservoir in the Northern Carnarvon Basin (Longley *et al.* 2002; Chongzhi *et al.* 2013; Geoscience Australia, 2017; Bilal *et al*. 2018). This study presents a subsurface evaluation of the western

Exmouth Plateau and associated fluid escape features affecting the Mesozoic plays in order to provide insights into the controls on fluid flow history within the basin dynamics.

A total of 171 fluid escape pipes were mapped and analysed in detail using a high-quality 3D seismic reflection data (Claudius 3D survey) from the western Exmouth Plateau, North West Shelf of Australia (Fig. 1). Velayatham *et al.* (2018) have published on a similar dataset of fluid escape pipes and focused their analysis on quantifying the linearity of the distribution of paleo-pockmarks and the possible structural control. This research represents an advance of this previous work by examining in detail the origin, distribution and morphological characteristics of the pockmarks and associated pipes. We further investigate the control on spatial distribution of the pockmarks and analyse and classify their associated fluid flow pipes.

Several studies have analysed and characterised fluid escape pipes (e.g. Cheng *et al*. 2020; Cartwright and Santamarina, 2015). In this study, fluid escape pipes were classified following the subdivision defined by Cartwright *et al.* (2007) as blowout, seepage, and hydrothermal pipes. Pipes and associated pockmarks were carefully evaluated using vertical sections integrated with seismic attributes along key stratigraphic surfaces. Particular attention was given to understanding the geometric and timing relationships between pipes and the prominent rift faults observed in the basin (Figs. 1b and c).

Geological setting of the Exmouth Plateau (B)

The Exmouth Plateau is an extensive marginal plateau located within one of world's most prolific hydrocarbon basins - the Northern Carnarvon Basin, North West Shelf of Australia (Chongzhi *et al.* 2013). The Northern Carnarvon Basin has experienced a multi-phase history of faulting since the Paleozoic (McCormack and McClay 2013; I'Anson *et al.* 2019; Deng and McClay 2019). The sedimentary infill of the basin is formed by ~15 km thick Phanerozoic shallow marine siliciclastics and shelfal carbonates (Fig. 2; Stagg and Colwell 1994; Rohead-O'brien and Elders 2018).

The breakup of eastern Gondwana during the Permo-Carboniferous involved a general north-west directed extension that initiated the formation of the Northern Carnarvon Basin and fundamentally controlled the later-stage evolution of the Mesozoic rift of the North West Shelf of Australia (Longley *et al.*2002; Gartrell 2000; Gartrell *et al.* 2016; Deng and McClay 2019). In the Exmouth Plateau, this resulted in a widespread deposition of marine sediments as shown in the stratigraphic chart in Figure 2 (AGSO, 1994; Pryer *et al.* 2014). Syn-rift basin infill of Early Permian glacio-fluvial sediments is overlain by Late Permian marine clastic and carbonate deposits (Longley *et al*. 2002). This was followed by a regional post-rift subsidence that accommodated the marine transgressive Lower to Middle Triassic Locker Shale that transitioned upwards into the thick Upper Triassic Mungaroo Formation (Fig. 2) (Longley *et al.* 2002; Gartrell 2000; Rohrman 2013; Black *et al.* 2017), where numerous fluid escape pipes are observed (Figs. 2 and 3). The Mungaroo Formation is composed of claystone, siltstones, sandstone, and coal sediments deposited by mainly fluvio-deltaic systems. The formation contains the key reservoir intervals (Fig. 2; Longley *et al.* 2002). Subsequent Late Triassic to Early Jurassic rapid subsidence resulted in the deposition of the Brigadier Formation and Murat Siltstone, which form an Early to Mid-Jurassic condensed succession of thinly bedded shelfal siltstone, claystone and marl (Fig. 2; Gartrell 2000; Longley *et al.* 2002; Gartrell *et al.* 2016; Bilal *et al*. 2018).

During the Middle to Late Jurassic, a major phase of rifting between Greater India and western Australia occurred in the north of the Northern Carnarvon Basin (Tindale *et al.* 1998; Stagg *et al.* 2004; Gartrell 2000). This phase focused in the eastern inner-board margin of the Exmouth Plateau, with only minor extension occurred in the plateau (Jitmahantakul and McClay 2013; Bilal *et al*. 2018). The syn-rift succession accumulated during this period consists of dominantly fine-grained marine sediments of the Athol Formation and Dingo Claystone, deposited in a low energy environment and ponding into the hangingwalls of rift structures (He and Middleton, 2002; Bilal *et al.* 2018). Jurassic extension was also accompanied by the emplacement of magmatic sills and dykes intruding the Mungaroo and younger formations (Fig. 1b and 3; Symonds *et al*. 1998; Stagg *et al.* 2004; McClay *et al*. 2013; Rohrman 2013; Black *et al.* 2017; Magee *et al.* 2017; 2020).

The Late Jurassic rifting culminated in seafloor spreading, subsequently forming the Argo abyssal plain to the northeast of the Exmouth Plateau at approximately 155 Ma (Muller *et al*. 1998; Longley *et al.* 2002; Heine and Muller 2005; McClay *et al.* 2013). Breakup was associated with a regional marine transgression and drove rapid and large subsidence with the deposition of the Barrow Group (Rohrman 2013) and influenced crustal extension and thinning of the basin (Barber 1988; Driscoll and Karner 1998; He and Middleton, 2002).

The regional Early Cretaceous Valanginian (K20.0_SB) erosional unconformity the marks a late rifting onset between Greater India and Australia (Figs. 1b, 2 and 3; Longley *et al.* 2002; Stagg *et al.* 2004; Black *et al*. 2017; Bilal *et al.* 2018) and seafloor spreading. The later lead to the opening of the Gascoyne (135 Ma) and the Cuvier (133 Ma) abyssal plains to the west and south of the Exmouth Plateau, respectively (Longley *et al*. 2002; Heine and Muller 2005; Gibbons *et al*. 2012; Black *et al*. 2017). The post-rift succession of the Muderong Shale, Windalia Radiolarite and Gearle Siltstone represent prograding shelfal and slope sediments from Late Cretaceous to Cenozoic with Paleogene and recent strata comprised of carbonate dominated sequences in the basin (Fig. 2; Hocking 1988; He and Middleton 2002).

By the Late Oligocene - Early Miocene, convergence between the Australian and Eurasian plates (Keep *et al.* 1998; Hall 2012; Cathro and Karner 2006) resulted in shallow extensional faulting across the Northern Carnarvon Basin causing tilting, inversion, and general widespread reactivation of the larger underlying Triassic to Early Cretaceous rift structures (Fig. 3; Cathro and Karner 2006; Hall 2013; Longley *et al*.2002; Van Tuyl *et al*. 2018).

Data and Methodology (B)

Seismic and well data (C)

This study used a time-migrated marine seismic reflection survey acquired in 2010 that covers a total full fold area of ~3750 km^2 (Claudius 3D survey; Fig. 1a). The survey is located in the western edge of the Exmouth Plateau at water depths ranging from 1400-2000m (Fig. 1). It has inline (east-west) and crossline (north-south) spacing of 12.7m and 18.8m, respectively. The data is zero-phased and processed following the Society of Exploration Geophysicists (SEG) European polarity convention, whereby a downward increase in acoustic impedance corresponds to a negative amplitude (black reflection); a decrease in acoustic impedance corresponds to a positive amplitude (red reflection). A dominant seismic frequency of 50 Hz and a velocity of ~3.3 km s^{-1} (Woodside, 2011b) yield a vertical seismic resolution of a proximately 16.5m at the interval of interest – a two-way time (TWT) of 2.5-4 seconds, which corresponds to the Upper Triassic to Early Cretaceous successions, where the fluid escape pipes are observed.

The stratigraphic framework adopted in this research was constrained using bio-stratigraphic markers from Eendracht-1 (Esso Australia 1981) and Alaric-1 (Woodside 2011a) wells (Fig. 1a). Nomenclature of key time surfaces is based on the work of Marshall and Lang (2013) on the regional stratigraphy of the North West Shelf of Australia.

Morphological analysis of fluid escape pipes (C)

As shown in the structural map of the Rhaetian TR30.1_TS, fluid escape pipes are mainly located on the eastern part of the survey, which is the focus of this research (Figs. 4 and 5). Fluid escape pipes are seismically interpreted as vertical to sub-vertical zones of disrupted reflections cutting through the stratal succession (Figs. 4b and c). Hence, lateral and vertical boundaries of fluid escape pipes were identified by the extent of such seismic disturbance of reflections (Fig. 4c). Seismic interpretation of pipes was mainly carried out using standard amplitude volumes. However, a coherency attribute was also used to aid the identification of pipes (e.g. Fig. 7) as it highlights discontinuous reflections (e.g. Li 2014).

In the study area, fluid escape pipes of variable sizes typically exhibit circular depression of disrupted seismic packages along the Rhaetian TR30.1_TS and Oxfordian J40.0_SB horizons (Fig. 4c). These erosive features were interpreted as pockmarks connected to a source at depth via the fluid escape pipes (Fig. 4). The pockmarks are exceptionally well-imaged at the Rhaetian TR30.1_TS level where they display clearer pipe openings than those observed at the Oxfordian J40.0_SB level. This is because the majority of fluid escape pipes affected TR30.1_TS and terminated at the J40.0_SB unconformity or slightly below. Thus, horizon TR30.1_TS was used to map the spatial distribution of fluid escape pipes in the survey area (Fig. 4a).

Once the location of the pipe openings was defined and mapped, vertical seismic sections were taken through these features in order to analyse the morphologies of associated fluid escape pipes. The following measurements were recorded (Fig. 4c):

- *Pipe conduit bottom (PiB):* Identified as the pipe root zone where the pipe bottom conduit reflections terminated (measured in TWT depth). This mesurement provides a proxi for the stratigraphic units where the interpreted pipes are sourced.
- *Pipe top (PiT):* Commonly, pipes terminate upwards with pockmarks (e.g. Fig. 4c). This measurement is the depth (TWT) of the top of such pockmarks. This measurement is important as it gives indication of the stratigraphic level where pipes terminated upwards, hence this provides constraints on the timing of formation of fluid escape pipes (Cartwright and Santamarina , 2015).
- *Pipe conduit length (PiL):* this was derived from the subtraction of the pipe top (PiT) and the pipe conduit bottom (PiB) to obtain a total length (TWT) of the pipes. These measurements were depth converted to meters using checkshot survey of Alaric-1 well (Woodside, 2011b). An average velocity of 3300m/s was considered for the upper section of the Mungaroo Formation where fluid escape pipes are observed.
- *Pipe diameter (PiD):* this is the maximum pipe column diameter. It was typically taken near the upper end of each pipe conduit since most pipes exhibited to be wider in their respective upper zones. Together with PiL (*Pipe conduit length)*, this is a key measurement that provide constraints for the morphology of the fluid escape pipes analysed in the study area.

Seismic stratigraphy (B)

The stratigraphy of the research area ranges from Triassic to recent. However, the study focuses on the Upper Triassic to Early Cretaceous succession where the fluid escape pipes are observed. This succession can be divided into three major tectono-stratigraphic megasequences and further subdivided into six units (Figs. 2 and 3; Table 1).

Pre-rift megasequence (155 Ma-250 Ma) (C)

Lower Norian and older (lower -Mungaroo Formation) (D)

Is the deepest in the area and mainly forms the lower part of the Mungaroo Formation (Fig. 2 and Table 1). The unit is bounded to the top by the TR22.4 seismic horizon which has variable continuity due to poor seismic imaging and extends to the bottom of the survey at 6s (TWT). The Eendracht-1 Well Report (1981) indicates that a third of the unit is composed of thick grey sandstones, and the rest by argillaceous siltstones with dark grey claystones identified as the deltaic sediments of the Mungaroo Formation.

These sediments are seismically imaged as low to high amplitude and continuous parallel reflections (Figs. 2 and 3). Several fluid escape pipes are rooted within this unit.

High amplitude reflections that transgress stratigraphy and show evidence of abrupt terminations are interpreted as igneous intrusions, including sills and local dykes. Sills occur mainly at depth of 5.9s (TWT) and extends ~5 km from west to east (Fig. 1). A number of fluid escape pipes are located above the sill indicating their hydrothermal genesis.

Middle to Upper Norian (upper Mungaroo Formation) (D)

This unit represents the upper part of the Mungaroo Formation and incorporates two regional high amplitude and continuous markers: TR26.1_TS in the middle section (above TR22.4_MFS), and the Intra-Triassic TR27.2_MFS maximum flooding surface which bounds this unit to the top(Figs. 2 and 3; Woodside a, 2011).

The section below the TR26.1_TS marker, displays parallel reflections with predominantly low amplitude responses representing the siltstones, calcareous claystones and minor sandstone (Esso Australia, 1981) of the Mungaroo Formation. Coarser material from this unit could be reflected in the few isolated medium amplitude reflections displayed in the seismic within Mungaroo Formation. The upper section of this unit (above TR26.1_TS) exhibits high-amplitude parallel reflections, potentially suggesting the presence of coarser material in the succession.

Uppermost Norian to Lower Rhaetian (Uppermost-Mungaroo Formation) (D)

This unit represents the uppermost part of the Mungaroo Formation and it is composed predominantly of siltstones and calcareous claystones with minor amounts of sandstone deposited in a shallow marine environment (Marshall and Lang*,* 2013). The transition to dominant marine sediments is displayed by parallel and continuous reflections with low amplitude at the bottom of the section and with variable amplitudes at the top (Fig. 3). The Mungaroo Formation is bounded to the top by the TR30.1_TS transgressive surface, which is displayed as a continuous, strong amplitude reflection across the survey area. Apart from the extensive fields of pockmarks analysed in this study, this surface also shows isolated carbonate mounds to the west of the survey area (Fig. 4a). These are seismically characterised by dome-shaped features and represent an Upper Triassic carbonate system (Grain *et al.* 2013).

Rhaetian to Oxfordian (D)

This unit is formed by packages of parallel reflections bounded by the Rhaetian TR30.1_TS transgressive surface at the bottom and by the Oxfordian J40.0_SB unconformity at the top (Fig. 3). The strata consist of thick dark grey claystones and marls of the Brigadier, Murat and Athol formations and lower Dingo Claystone (Marshall *and Lang* 2013). This unit is where most of the fluid escape pipes seem to terminate.

Syn-rift megasequence (155 Ma-140 Ma) (C)

Oxfordian to Valanginian (D)

The unit shows strongly wedging and fanning growth strata of the syn-rift megasequence with variable amplitudes. Overall, the unit thicken in the hangingwalls of the N-S to NNE-SSW extensional faults and extend from the J40.0_SB Oxfordian unconformity to the K20.0_SB Valanginian unconformity. It consists of the Dingo Claystone and Barrow Group (Figs. 2 and 3).

Post-rift megasequence (140 Ma – present) (C)

Valanginian to Cenozoic (D)

Dominant carbonate and minor clastics characterise this succession. The unit is bounded by the Valanginian K20.0_SB unconformity at the bottom and by the seabed at the top (Fig. 3). The lower section exhibits parallel and continuous reflections with low to medium amplitude responses heavily affected by polygonal faults (Fig. 3).

Main structures (B)

The pre and syn-rift megasequences (Table. 1) where fluid escape pipes were interpreted, are affected by a series of well-developed, N-S to NNE-SSW-oriented planar extensional fault arrays with associated growth strata in their hanging-wall basins (Fig. 3). Major faults are affected by footwall-scarp degradation and exhibit complex linkage pattern along both strike and dip (Figs. 3 and 4). Hanging-wall basins are underfilled and segmented along strike (Fig. 4). Most of the faults terminate below the Valanginian K20.0_SB unconformity. Extensive polygonal faults occur in the carbonate dominated sediments of the Valanginian to recent post-extension sequences. Polygonal faults and reactivated extensional faults appear to be the youngest structural element as they are restricted to the post-extension sequence (Fig. 3).

Half-graben array (C)

The structural style of the research area is typically characterised by domino-style, planar extensional faults that form half-grabens up to 10 km width with an overall NNE-SSW trend (mean strike trend 022; Figs. 5a and 5b). Within the half-grabens, fanning strata geometries representing syn-rift growth strata are observed (Fig. 3). The age of the growth strata is interpreted to be Oxfordian to Valanginian, indicating a major phase of extension in the area from the Late Jurassic to Early Cretaceous (Fig. 3). The upper tip of half-grabens bounding faults terminates predominately below the Valanginian K20.0_SB unconformity while the lower tip extends beyond the bottom limit of seismic data. Some of the bounding faults propagate upwards, refract within the Cenozoic strata and, in places, links vertically with the polygonal faults (Fig. 3). This evidence indicates that the half-graben-bounding fault array was reactivated in the Cenozoic.

Minor intra-graben array (C)

A series of dominantly east dipping, domino-style planar extensional faults form minor intra graben faults with a dominant NNW-SSE trend (mean strike trend 338°; Figs. 3, 5a and 5b). These faults exhibit complex early linkage structures and their NNW-SSE trend is consistent with the spatial alignment of the pockmarks interpreted in this study (Fig. 5). The upper tip of the faults terminates within the upper Jurassic syn-extension strata while the lower tip terminates within the uppermost Triassic strata.

Characterisation of fluid escape pipes (B)

Classification (C)

In this research, a total of 171 fluid escape pipes were identified and classified into blowout (140), seepage (26) and hydrothermal (5) pipes. Blowout pipes are the most common type, contributing 82% of the total pipes (Fig. 6a). Whereas 15% of fluid escape pipes were identified as seepage being scattered in the study area and commonly found together with blowout pipes (Fig. 5a and 6a). Hydrothermal fluid escape pipes comprise only 3% of the pipes, making these the least common type of pipes in the study area (Fig. 6a). These pipes are spatially related to igneous sills at depth, with the root zone of hydrothermal pipes within the Lower Norian and older unit (Fig. 1).

Spatial analysis and relation to fault arrays (C)

All three types of fluid escape pipes were widely distributed across the study area (Fig. 5a). Typically, fluid escape pipes were found in clusters aligned parallel to sub-parallel to the minor NNW-SSE-trending intra-graben fault array in trails up to 39 km long arranged in an overall NNW-SSE (338°) trend (Fig. 5 a and 5b). Few pipes, however, were found as isolated features, unrelated to the fault arrays (Fig. 5c).

Fluid escape pipes appeared to cross-cut pre-existing fault planes as they extended upward from their root zone with blowout pipes displayed this occurrence the most. The pipes nucleate at or near fault planes with pockmarks at or near Late Jurassic Oxfordian J40.0_SB unconformity. More than half of the pipe population was identified rooting from graben bounding faults and from the minor intra-graben fault arrays (Fig. 5c and 7).

Morphological analysis (C)

The pipe population exhibit an average diameter of 115 m (Fig. 6b). Hydrothermal pipes have the largest diameters (> 200m) followed by blowout pipes and seepage pipes with average diameter of ~100m (Fig. 6b). Strikingly, most of the pipe population was found to have their top terminus at narrow depth interval of 3-3.2s (TWT; Fig. 6b). This depth is regionally correlated to J40.0_SB Oxfordian horizon (Fig. 8). In contrast, the root zone of the blowout, seepage and hydrothermal pipes was found at different depths indicating multiple fluid sources at different stratigraphic levels in the Triassic and older strata, typically at depth interval from 3.4s to 6s (TWT) (Figs. 6e and 7). Within this depth range, distinct frequency maxima can be identified (Fig. 6e) - one in the Upper Norian at 3.8s (TWT), and three in the Lower Norian and older at 4.2s (TWT), 4.6s (TWT), and 5.6s (TWT). Figure 7 displays examples of blowout pipes rooting at these different stratigraphic levels.

Pipe length (D)

Fluid escape pipes displayed a wide range of lengths, thus, they were categorised into short (≤1500 m), medium (<3000 m), and long (≥3000 m) pipes. Over 50% of the pipe population length was found to be short, with the shortest being a seepage pipe ~80 m long. 35% of pipes were medium and just over 10% was categorised as long pipes. The longest pipe is a hydrothermal pipe exceeding 4.5 km in length (Fig. 6d). Overall, seepage pipes are prominently short, blowout pipes tend to be short to medium, and hydrothermal pipes were found to be the longest (Fig. 6d).

Discussion (B)

Fluid escape pipes, Jurassic extension and magmatism (c)

The wedge-shaped growth strata found in the hanging-walls of the half-graben array in the study area is interpreted to form a syn-rift sequence that is constrained between the J40.0_SB Oxfordian and K20.0_SB Valanginian unconformities (Fig. 3). This implies that the main extension in the western Exmouth Plateau occurred at that time (Fig. 8). The extensional event well conforms with studies of Heine and Müller (2005), Longley *et al.* (2002) and Marshall and Lang (2013) who proposed a Late Jurassic rift that culminated with the initiation of the Argo seafloor spreading at ~155 Ma.

Since the J40.0_SB Oxfordian unconformity represents the onset of rifting and also is where the top terminus of the pipe population was found (Fig. 5a, 7b and 10), it is proposed that fluid escape pipes formed at the beginning of the main rifting phase in the Late Jurassic, subsequent to the formation of the Oxfordian unconformity (J40.0_SB) and prior to the development of the Valanginian unconformity (K20.0_SB). Thus, the timing of pockmarks formation is roughly constrained between Oxfordian and Berriasian, slightly earlier than the interpretation of Velayatham *et al.* (2018) (Fig. 9). The different direction of the two rift fault arrays (i.e NNW-SSE-trending minor intra-graben and NNE-SSW-trending half-graben array) indicates that these two trends have possibly formed at different times (Fig. 5b and 9). Pockmarks and underlying pipes are interpreted to have no relation to the NNE-SSW trending, dominantly west-dipping major extensional faults. However, they are strongly aligned with a series of low displacement, NNW-SSE-trending intra-graben faults (Fig. 5). Fluid flow features in the Exmouth Plateau are commonly interpreted to form linear trends that are parallel to the low displacement intra-rift faults that trend to both NNE-SSW and NNW-SSE (e.g. Velayatham *et al.* 2018; 2019; Bilal 2019).

Fluid escape pipes displayed a wide range of lengths, with blowout and hydrothermal pipes associated to the deep overpressured layers, where fluid pressure was likely the highest. According to Leduc *et al.* (2013) fluid escape pipes found in the Niger Delta were also identified with several lengths and diameters which genesis involved hydraulic fracturing of the overburden. The authors noted that fluid escape pipe genesis involved lateral pressure transfer from channel complexes rooting from the crest of anticlines. In the study, area of this research the pipe population was found rooting from different stratigraphic sources within the Mungaroo Formation (Figs. 6e, 8 and 9). Thus, we infer that faulting associated with the NNW-SSE-trending intra-graben array resulted in the breach of multiple overpressured layers that were present at different stratigraphic levels within this formation. Extensional tensile stresses, developed during rifting, may have also increased buoyancy in the overpressured layers of the Mungaroo Formation inducing hydraulic fracturing in the root zone of fluid escape pipes. This led to vertical fluid migration resulting in genesis of fluid escape pipes towards the J40.0_SB paleo-seabed prior deposition of the Dingo Claystone and Barrow Group sediments (Fig. 2). We propose that in the Exmouth Plateau soon after breaching, pipes became inactive as fluid pressure was released as shown by the lack of pipes in the strata immediately above the Oxfordian unconformity (Fig. 9).

Hydrothermal pipes result from the intrusion of sills into porous sedimentary rocks and release of pore-waters and magmatic fluids (Figs. 9 and 10; Holford et al. 2013). In the study area, since these pipes were also found terminating at the J40.0_SB horizon, we suggest that magmatic activity here coincided with the Late Jurassic extensional phase (Figs. 9 and 10). These findings are in a agreement with Rohrman (2013), Holford *et al.* (2013) and Bilal (2019) who proposed that, in the Exmouth Plateau, igneous intrusions were emplaced during the Late Jurassic to the Early Cretaceous. Our study suggests that igneous activity was short-lived and constrained within the Late Jurassic as indicated by the termination of hydrothermal pipes at the Oxfordian unconformity.

Morphology and genesis of fluid escape pipes (C)

It is proposed that high levels of overpressures sustained the propagation of blowout pipes since these are rooting from deeper stratigraphic levels of the Mungaroo Formation and also displayed wider and larger conduits (Fig. 6b, 6d and 6e). Uplift of fluids under conditions of high pressure in blowout pipes is supported by the fact that commonly these pipes exhibit prominent pockmarks at the upper terminus, which might indicate explosive release of fluids at the paleo-seabed. Blowout pieps have also been identified in the North Sea (Maestrelli et al. 2017) and several other studies including Palan *et al.*(2020), Loseth *et al.*(2011) and Traynor and Sladen (1997) who have given evidence and supported the explosive genesis of associated pockmarks. Since blowout dominate the study area, this implies that Triassic sources of fluids in the Exmouth Plateau must have been highly overpressured.

Seepage pipes terminate in mounds lacking a violent outburst of fluid to generate pockmarks as Cartwright *et al.* (2007) proposed. It is argued that seepage pipes form under relatively less pressure than blowout pipes which outlines their major difference. This is supported by morphological results of our study displaying seepage pipes being narrower with shorter lengths and sourcing from shallower root zones (Fig. 6b, 6d and 6e).

Hydrothermal pipes are the longest and wider pipes in the study area (Fig. 6b and 6d). We propose that magmatic activity in the Late Jurassic syn-extension lead to an increase of lithostatic pressure due to the emplacement of igneous sills at depth. Such resulted in a large and greater vertical outburst of magmatic fluid flux and fracture of the pore network. Therefore, the genesis of these pipes involves greater pressure changes and higher fluid outburst.

Controls on fluid escape pipe occurrence and overpressure (c)

Pipe-fault spatial relation (D)

The NNW-SSE-oriented intra-graben minor faults and fluid flow features interpreted in this research have a strong spatial relationship (Fig. 4). Pockmarks and their underlying fluid escape pipes have been interpreted to lie within highly linear NNW-SSE pockmarks trains, which are parallel to sub-parallel to the NNW-SSE-oriented minor intra-graben extensional faults (Fig. 5a and 5b). These faults have been interpreted to have formed during the Late Jurassic (Oxfordian) to Early Cretaceous (Valanginian) rifting of the Exmouth Plateau. Breaching of one, or multiple overpressured source layers within the pre-rift Mungaroo Formation during rifting by the formation of the intra-graben faults not only triggered the formation of fluid escape pipes, but also caused the extraordinary long (39 km) and linear trains of the pockmarks observed at the Rhaetian (TR30.1 SB) and Oxfordian (J40.0 SB) levels (Figs. 5a, 5c, 9 and 10).

Depending on the local mechanical characteristic of fault damage zones, fluids may or may have not used faults as migration pathways prior vertical propagation towards the paleoseabed (Fig. 10 and 11). Similar relations of fluid escape pipes have been observed in the North Sea, where these were described as 'channel-like features' resulting from hydrothermal venting of their magmatic fluids during intrusion (Underhill 2009). Structural control of faults on pockmarks distribution and focused fluid flow has also been documented in the northern Gulf of Mexico (Roelofse *et al.* 2019), offshore Angola (Maia *et al.* 2016) and South China (Wang *et al,* 2019).

In this research, the isolated blowout and seepage pipes (Figs. 5a, 10 and 11), and respective root zones, were not found related to the fault arrays. It is envisaged that minor faults and fractures (below the seismic resolution of ~16.5m) may have initiated these isolated pipes. Alternatively, they might have been originated by sills at depths, not imaged by the 3D seismic survey (Fig. 10).

Hydrothermal activity (D)

Hydrothermal pipes were found rooting at great depths from sills and possible dykes (i.e. Magee *et al.* 2020) in the Lower Norian unit and showing the longest conduits (Fig. 7). Some pipes extend beyond the lower boundary of the seismic dataset, suggesting deeper sources, potentially from deep sills. It is known that hydrothermal fluids are derived from devolatilization of magma and from the host sediments by localised heating and metamorphism (Cartwright et al. 2007; Cartwright and Santamarina 2015). These are likely the sources of fluids related with the hydrothermal pipes mapped in the area. Igneous intrusion-induced hydrothermal vents have also been recognised in other parts of the Exmouth Plateau (e.g. Bilal 2019; Magee *et al.* 2020) where fluid was released from the sills, ascended through the overlying Triassic and Jurassic strata, before being expelled in the Late Jurassic, post the Oxfordian J40.0 SB unconformity.

Hydrocarbon generation and formation of overpressure (D)

Models of overpressuring by gas generation have supported an increase in volume of pore pressure leading to generation of overpressure in closed systems (Hansom and Lee, 2014). Fluid migration is related to the release of overpressure due to hydrocarbon expulsion from source rocks (Judd and Hovland 2007; Cheng *et al*. 2020). Therefore, hydrocarbon release and volume expansion can lead to the excess overpressure and would favour fluid escape pipe genesis (Fig. 11a and 11b). Formation of overpressured layers due to hydrocarbon generation have been documented in the Niger Delta (Cobbold *et al.* 2004) and in the Baram Delta (Tingay *et al.*2009). In the Exmouth Plateau, overpressure might have been produced from the generation and maturation of abundant organic matter within the Triassic Mungaroo Formation shales (Fig. 11a; Barber, 1988; Swarbrick, 2002). Heat flow models calibrated to well data from Jarvis and Mckenzie (1980) and He and Middletone (2002) indicate that a main phase of hydrocarbon generation and accumulation took place in the Triassic Mungaroo Formation during the main rifting event in the Oxfordian (Fig. 9). Thermal modelling by Barber (1988) and vitrinite reflectance measurements by Cook *et al.* (1985) suggests that the hydrocarbon generation began in the Late Triassic to Early Jurassic, through the Tertiary. This studies above might support that hydrocarbon-bearing overpressured layers were being charged since the Late Triassic (Fig. 9) and were subsequently beached by Late Jurassic rift fault resulting in the formation of fluid escape pipes (Fig. 11).

Implications for hydrocarbon exploration (C)

Hydrocarbon charge across the Exmouth Plateau is sourced from organic-rich shales and the coal-rich beds of the Triassic Mungaroo Formation. The main reservoir units are the sand-prone facies of the Triassic Mungaroo Formation, the Upper Triassic carbonate buildups of the Brigadier Formation and the Early Cretaceous Barrow Group (Grain *et al.* 2013; Chongzhi 2013; Marshall and Lang 2013; Geoscience Australia, 2017). Although the Mungaroo Formation constitutes intra-formational seals, the Early Cretaceous marine Shale acts as a regional seal in the area (e.g. Chongzhi et al. 2013).

Fluid escape pipes are important for hydrocarbon exploration as they provide insights into reservoir location, play a critical role in fluid migration pathways, and constitute risks for seal integrity (e.g. Andresen, 2012). It is therefore fundamental in hydrocarbon exploration to understand the effect that fluid escape pipes might have in a basin. Pockmarks are also commonly used to evidence the occurrence or leakage of deeper petroleum systems (Hovland and Judd, 1988; Andresen *et al.* 2011), hence, fluid escape pipes can be used as indicators of hydrocarbon presence (e.g. Heggland 2005; Andresen 2012).

In the study area, the occurrence of numerous fluid escape pipes (Fig. 5a) might suggest expulsion of potential hydrocarbons sourced from the Mungaroo Formation into the Jurassic strata (Fig. 10, 11b and 11c). Furthermore, fluid escape pipes represent a risk for the seal integrity for the Mungaroo Formation and migration pathways to Jurassic and Early Cretaceous plays. Evidence of hydrocarbon seepage from deep reservoirs is widely reported across the Exmouth Plateau (e.g. Jablonski et al. 2013; Paganoni *et al.* 2019). The potential presence of igneous features and related structures (i.e. Magee *et al.* 2020) within the Mungaroo Formation helps to better assess the stability in the area and analyse these structures as potential geohazards for exploration in the western Exmouth Plateau.

Petroleum exploration in the area (Fig. 1a) displayed variable hydrocarbon levels: Alaric-1 discovered a 185m gas column (Woodside, 2011a), Eenchdrach-1 a net section of 25m, Cadwallon-1 a 27m gross hydrocarbon column (Woodside, 2011), and Tiberius-1 and Genseric-1 appeared dry (Geoscience Australia, 2017). Geoscience Australia (2017) has concluded that the lack of hydrocarbons found is due to the eroded Jurassic strata that could not provide a suitable seal for the system. Nonetheless, it is suggested that hydrocarbons not only migrated during the early hydrocarbon generative phase in the Late Triassic (Barber, 1982), but also potential uplift of hydrocarbons through fluid escape pipes occurred in the early stage of rift, when traps were likely not fully formed (Fig. 9). Hydrocarbon accumulation is also likely to have been impacted by the multiphase tectonic history of the area that might have resulted in episodic charging and seal breach.

Alaric-1, Eenchdrach-1 and Cadwallon-1 have found gas discoveries in the study area, therefore, we argue that hydrocarbon maturation continued during the Late Jurassic rifting, potentially aided by fluid escape pipes that acted as conduits from breached sourced hydrocarbon layers leading to migration and trapping within the tilted Mesozoic fault blocks. This would encourage exploration in the area around pipes surrounding viable trapping structures.

Conclusions (B)

The Triassic and Jurassic successions of the Mungaroo Formation in the western Exmouth Plateau is heavily affected by fluid escape pipes and related pockmarks. Analyses of high-quality seismic data revealed three types of fluid escape pipes: blowout are the most common pipes found, followed by seepage pipes and hydrothermal pipes. All fluid escape pipes have possibly formed at the same time during the early stages of rifting in the Late Jurassic. Analysis of fault-pipes timing relationships suggests that a main Late Jurassic rift-related extensional event caused breaching of overpressured layers in the basin. Consequent hydraulic fracturing produced vertical outburst of fluid towards the J40.0_SB Oxfordian unconformity, thus, creating NNW-SSE-trending clustered fluid escape pipes aligned parallel to sub-parallel to the intra-graben rift structures. The NNE-SSW major faults are interpreted to have no relation to the formation of the pockmarks and fluid escape pipes.

Different overpressure magnitudes likely controlled the morphology of fluid escape pipes. Deep, highly overpressured sources originated long and wide explosive pipes with well-developed pockmarks at their upper end - e.g. hydrothermal and blowout pipes. Shallow rooting pipes with limited pressure drive resulted in short seepage pipes terminating in mounds. Pipes rooting at different depths indicate the presence of overpressured layers at different stratigraphic levels in the Mungaroo Formation. Such overpressures were likely developed from hydrocarbon generation during the Triassic (blowout and seepage pipes) and by emplacement of igneous intrusions at the time of rifting (hydrothermal pipes). These features can operate as conduits for potential reservoir charge of the shallow reservoirs in the upper part of the Triassic Mungaroo Formation. This encourage exploration around fluid escape pipes intercepting viable rift-related traps.

Acknowledgements (B)

Geoscience Australia are thanked for providing the seismic data used in this research as part of a collaboration agreement with the Fault Dynamics Research Group, Department of Earth Sciences, Royal Holloway University of London. The seismic interpretation software, including DecisionSpace Desktop and Geoprobe was kindly provided by Halliburton Ltd. We finally thank Joe Cartwright and anonymous reviewer for their time and effort in providing through and constructive reviews of the manuscript and the editor Giovanni Camanni for his time and support.

References (B)

AGSO NORTH WEST SHELF STUDY GROUP, 1994. Deep reflections on the North West Shelf: changing perceptions of basin formation. Petroleum Exploration Society of Australia.

ANDRESEN, K.J., HUUSE, M., SCHØDT, N.H., CLAUSEN, L.F. AND SEIDLER, L., 2011. Hydrocarbon plumbing systems of salt mini basins offshore Angola revealed by three-dimensional seismic analysis. American Association of Petroleum Geologists Bulletin Vol. 95.6, p. 1039-1065.

ANDRESEN K.J., 2012. Fluid flow features in hydrocarbon plumbing systems: what do they tell us about the basin evolution? Marine Geology, p. 1-20.

BARBER, P.M., 1982. Palaeotectonic evolution and hydrocarbon genesis of the central Exmouth Plateau. The APPEA Journal, Vol. 22.1, p.131-144.

BARBER, P.M., 1988. The Exmouth Plateau deep water frontier: a case history. The North West Shelf, Australia, p.173-187.

BILAL, A., MCCLAY, K. AND SCARSELLI, N., 2018. Fault-scarp degradation in the central Exmouth Plateau, North West Shelf, Australia. Geological Society, London, Special Publications, 476, pp. SP476-11.

BILAL, A. 2019. Tectonostratigraphic evolution of the central Exmouth Plateau, North West Shelf, Australia. Unpublished doctoral Thiess. Royal Holloway, University of London. UK. p. 530

BLACK, M., MCCORMACK, K.D., ELDERS, C. AND ROBERTSON, D., 2017. Extensional fault evolution within the Exmouth Sub-basin, North West Shelf, Australia. Marine and Petroleum Geology, Vol. 85, p. 301-315.

CARTWRIGHT, J., HUUSE M. AND APLIN, A., 2007. Seal bypass systems. American Association of Petroleum Geologists Bulletin, Vol. 91, p. 1141-1166.

CARTWRIGHT, J. AND SANTAMARINA, C., 2015. Seismic characteristics of fluid escape pipes in sedimentary basins: implications for pipe genesis. Marine and Petroleum Geology, Vol. 65, p.126-140.

CATHRO, D.L. AND KARNER, G.D., 2006. Cretaceous–Tertiary inversion history of the Dampier Sub-basin, northwest Australia: insights from quantitative basin modelling. Marine and Petroleum Geology, Vol. 23.4, p.503-526.CHENG, C., JIANG, T., KUANG, Z., YANG, C., ZHANG, C., HE, Y., and XIONG, P. (2020). Characteristics of gas chimneys and their implications on gas hydrate accumulation in the Shenhu area, northern South China Sea. *Journal of Natural Gas Science and Engineering*, 103629.

CHONGZHI, T., GUOPING, B., JUNLAN, L., CHAO, D., XIAOXIN, L., HOUWU, L., DAPENG, W., 2013. Mesozoic lithofacies palaeogeography and petroleum prospectivity in North Carnarvon Basin, Australia. J. Paleogeograph. 2, 81–92. https://doi.org/10.3724/SP.J.1261.2013.00019

DAVIES, R.J. AND CLARKE, A.L., 2010. Methane recycling between hydrate and critically pressured stratigraphic traps, offshore Mauretania. Geology, Vol. 38, p. 963-966.

COBBOLD, P. R., MOURGUES, R., and BOYD, K. (2004). Mechanism of thin-skinned detachment in the Amazon Fan: assessing the importance of fluid overpressure and hydrocarbon generation. *Marine and petroleum geology*, *21*(8), 1013-1025.

COOK, A. C., SMYTH, M., and VOS, R. G. (1985). Source potential of Upper Triassic fluvio-deltaic systems of the Exmouth Plateau. *The APPEA Journal*, *25*(1), 204-215.

DENG, H., MCCLAY, K., 2019. Tectono-stratigraphy of the Dampier sub-basin, North West Shelf of Australia. In: MCCLAY, K.R., HAMMERSTEIN, J.A. (Eds.), Geological Society, London, Special Publications, Passive Margins: Tectonics, Sedimentation and Magmatism. Geological Society, London, Special Publications, vol. 476.

DRISCOLL, N.W. AND KARNER, G.D., 1998. ´Lower crustal extension across the Northern Carnarvon basin, Australia: Evidence for an eastward dipping detachment´. Journal of Geophysical Research: Solid Earth, Vol. 103-B3, p. 4975-4991.

ESSO AUSTRALIA, 1981. Well completion report Eendracht-1. Geoscience Australia, Government of Australia.

EXON, N.F., HAQ, B.U. AND VON RAD, U., 1992. Exmouth Plateau revisited: scientific drilling and geological framework. In Proceedings of the Ocean Drilling Program, Scientific Results, Vol. 122, p. 3-20.

Foschi, M., and Cartwright, J. A. (2020). Seal failure assessment of a major gas field via integration of seal properties and leakage phenomena. AAPG Bulletin, 104(8), 1627-1648.

GARTRELL, A., TORRES, J., DIXON, M., KEEP, M., 2016. Mesozoic rift onset and its impact on the sequence stratigraphic architecture of the Northern Carnarvon Basin. APPEA J. 56, 143–158.

GARTRELL, A.P. 2000. Rheological controls on extensional styles and the structural evolution of the Northern Carnarvon Basin, North West Shelf, Australia. Australian Journal of Earth Sciences, 47, 231–244.

GAY, A., LOPEZ, M., BERNDT, C. AND SERANNE, M., 2007. Geological controls on focused fluid flow associated with seafloor seeps in the Lower Congo Basin. Marine Geology, Vol. 244.1, p.68-

GEOSCIENCE AUSTRALIA 2017. Offshore Petroleum Exploration Acreage Release: Australia 2017. [online] Available at: http://www.petroleum-acreage.gov.au/2017/geology/northern-carnarvon-basin/western-exmouth-plateau [Accessed 18 May 2017].

GIBBONS, A.D., BARCKHAUSEN, U., DEN BOGAARD, P., HOERNLE, K., WERNER, R., WHITTAKER, J.M. AND MÜLLER, R.D., 2012. Constraining the Jurassic extent of Greater India: Tectonic evolution of the West Australian margin. Geochemistry, Geophysics, Geosystems, Vol. 13.5.

GRAIN, S.L., PEACE, W.M., HOOPER, E.C.D., MCCARTAIN, E., MASSARA, P.J., MARSHALL, N.G., LANG, S.C., 2013. Beyond the Deltas: Late Triassic Isolated Carbonate Build-ups on the Exmouth Plateau, 504 Carnarvon Basin, Western Australia, West Australian Basins Symposium 2013 Proceedings. 505 Petroleum Exploration Society of Australia, Perth, Western Australia.

HALL, R. 2012. Late Jurassic–Cenozoic reconstructions of the Indonesian region and the Indian Ocean. Tectonophysics, 570, 1–41, https://doi.org/10.1016/j.tecto. 2012.04.021

HALL, R., 2013. Contraction and extension in northern Borneo driven by subduction rollback. Journal of Asian Earth Sciences, Vol. 76, p.399-411.

HANSOM, J., and LEE, M. K. (2005). Effects of hydrocarbon generation, basal heat flow and sediment compaction on overpressure development: a numerical study. Petroleum Geoscience, 11 (4), 353-360.

HASKELL, N., NISSEN, S., HUGHES, M., GRINDHAUG, J., DHANANI, S., HEATH, R., KANTOROWICZ, J., ANTRIM, L., 519 CUBANSKI, M., NATARAJ, R., SCHILLY, M., WIGGER, S., 1999. Delineation of geologic drilling hazards using 520 3-D seismic attributes. The Leading Edge 18, 373-382.

HE, S. AND MIDDLETON, M., 2002. Heat flow and thermal maturity modelling in the northern Carnarvon Basin, North West Shelf, Australia. Marine and Petroleum Geology, Vol. 19.9, p. 1073-1088.

HEGGLAND, R., 2005. Using gas chimneys in seal integrity analysis: A discussion based on case histories. The American Association of Petroleum Geologists. AAPG Hedberg Series no. 2, p. 237-245.

HEINE, C. AND MÜLLER, R.D., 2005. Late Jurassic rifting along the Australian North West Shelf: margin geometry and spreading ridge configuration. Australian Journal of Earth Sciences, Vol. 52.1, p. 27-39.

HOCKING, R.M., 1988. Regional geology of the northern Carnarvon Basin. The North West Shelf, Australia, Proceedings of Petroleum Exploration Society of Australian Symposium, Perth, Western Australia, p. 97-114.

HOLFORD, S.P., SCHOFIELD, N., JACKSON, C.L., MAGEE, C., GREEN, P.F. AND DUDDY, I.R., 2013. Impacts of igneous intrusions on source reservoir potential in prospective sedimentary basins along the western Australian continental margin. Journal of Geophysical Research, Solid Earth, Vol. 118, p. 4477-4487.

HOVLAND, M., JUDD, A.G., 1988. Seabed Pockmarks and Seepages. Graham and Trotman, London.

I'ANSON, A., ELDERS, C., MCHARG, S., 2019. Marginal fault systems of the northern Carnarvon Basin: evidence for multiple palaeozoic extension events, north-West Shelf, Australia. Mar. Pet. Geol. 101, 211–229

JARVIS, G.T. AND MCKENZIE, D.P., 1980. Sedimentary basin formation with finite extension rates. Earth and Planetary Science Letters, Vol. 48.1, p.42-52.

JITMAHANTAKUL, S., MCCLAY, K., 2013. Late Triassic – Mid-Jurassic to Neogene Extensional Fault Systems in the Exmouth Sub-Basin, Northern Carnarvon Basin, North West Shelf, Western Australia, in:KEEP, M. and MOSS, S.J. (Eds), 2013, The Sedimentary Basins of Western Australia IV: Proceedings of the Petroleum Exploration Society of Australia Symposium. Perth.

KEEP, M., POWELL, C.M. and BAILLIE, P.W. 1998. Neogene deformation of the North West Shelf, Australia. In: PURCELL, P.G. and PURCELL, R.R. (eds) The Sedimentary Basins of Western Australia II. Proceedings of Petroleum Exploration Society Australia Symposium. Petroleum Exploration Society of Australia, Perth, Australia, 81–91.

JUDD, A., and HOVLAND, M. (2009). Seabed fluid flow: the impact on geology, biology and the marine environment. Cambridge University Press.

KARNER, G.D. AND DRISCOLL, N.W., 1999. Style, timing, and distribution of tectonic deformation across the Exmouth Plateau, northwest Australia, determined from stratal architecture and quantitative basin modelling. Geological Society, London, Special Publications, Vol. 164.1, p.271-311

LEDUC, A. M., DAVIES, R. J., SWARBRICK, R. E., and IMBER, J. (2013). Fluid flow pipes triggered by lateral pressure transfer in the deepwater western Niger Delta. Marine and Petroleum Geology, 43, 423–433. https://doi.org/10.1016/j.marpetgeo.2012.12.005

LI, M., 2014. Geophysical exploration technology: Applications in lithological and stratigraphic reservoirs. Elsevier, Chapter 3

LIGTENBERG, J.H., 2005. Detection of fluid migration pathways in seismic data: implications for fault seal analysis. Basin Research, Vol. 17.1, p.141-153

LONGLEY, I.M., BUESSENSCHUETT, C., CLYSDALE, L., CUBITT, C.J., DAVIS, R.C., JOHNSON, M.K., MARSHALL, N.M., MURRAY, A.P., SOMERVILLE, R., SPRY, T.B. AND THOMPSON, N.B., 2002, The North West Shelf of Australia - a Woodside Perspective. The Sedimentary Basins of Western Australia 3: Proceedings of the Petroleum Exploration Society of Australia Symposium, Perth, WA, p. 28–88.

LØSETH, H., GADING, M. AND WENSAAS, L., 2009. Hydrocarbon leakage interpreted on seismic data. Marine and Petroleum Geology, Vol 26.7, p. 1304-1319

LØSETH, H., WENSAAS, L., ARNTSEN, B., HANKEN, N. M., BASIRE, C., and GRAUE, K., 2011. 1000 m long gas blow-out pipes. Marine and Petroleum Geology, 28, 1047-1060

MAESTRELLI, D., IACOPINI, D., JIHAD, A.A., BOND, C.E., BONINI, M., 2017. Seismic and structural characterization of fluid escape pipes using 3D and partial stack seismic from the Loyal Field (Scotland, UK): a multiphase and repeated intrusive mechanism. Mar. Petrol. Geol. 88, 489–510. https://doi.org/10.1016/j.marpetgeo.2017.08.016

MAGEE, C., DUFFY, O.B., PURNELL, K., BELL, R.E., JACKSON, C.A.L. and REEVE, M.T. 2015. Fault-controlled fluid flow inferred from hydrothermal vents imaged in 3d seismic reflection data, offshore NW Australia. Basin Res., 20, 299–318

MAGEE, C., JACKSON, C. A. L., HARDMAN, J. P., and REEVE, M. T. (2017). Decoding sill emplacement and forced fold growth in the Exmouth Sub-basin, offshore northwest Australia: Implications for hydrocarbon exploration. Interpretation, 5(3), SK11-SK22.

MAGEE, C. and JACKSON, C.A.L. 2020. Seismic reflection data reveal the 3D structure of the newly discovered Exmouth Dyke Swarm, offshore NW Australia. Solid Earth, 11, 579–606. https://doi.org/10.5194/se-11-579-2020

MAIA, A.R., CARTWRIGHT, J., ANDERSEN, E., 2016. Shallow plumbing systems inferred from spatial analysis of pockmark arrays. Mar. Petrol. Geol. 77, 865–881.

MCCLAY, K., SCARSELLI, N. AND JITMAHANTAKUL, S., 2013. ´Igneous intrusions in the Carnarvon Basin, NW Shelf, Australia. In The sedimentary basins of Western Australia´ IV: Proceedings of the Petroleum Exploration Society of Australia Symposium: Perth, Petroleum Exploration Society of Western Australia, p. 1-20.

MCCORMACK, K.D. and MCCLAY, K. 2013. Structural architecture of the Gorgon Platform, North West Shelf, Australia. In: KEEP, M.and MOSS, S.J. (eds) The Sedimentary Basins of Western Australia IV.

Proceedings of Petroleum Exploration Society of Australia Symposium. Petroleum Exploration Society of Australia, Perth, Australia, 18–21

MOSS, J.L. AND CARTWRIGHT, J.A., 2010. The spatial and temporal distribution of pipe formation, offshore Namibia. Marine and Petroleum Geology, Vol. 27, p. 1216-1234.

MÜLLER, R.D., MIHUT, D. AND BALDWIN, S., 1998. A new kinematic model for the formation and evolution of the west and northwest Australian margin. The sedimentary basins of Western Australia, Vol. 2, p. 55-72.

OMOSANYA, K.O., MAIA, A.R. and ERUTEYA, O.E. 2020. Seismic, morphologic and scale variabilities of subsurface pipes and vent complexes in a magma-rich margin. Bull Volcanol 82, 40. https://doi.org/10.1007/s00445-020-01379-3

OSBORNE, M.J. AND SWARBRICK, R.E., 1997. Mechanisms for generating overpressure in sedimentary basins: a reevaluation. AAPG bulletin, Vol. 81.6, p. 1023-1041.

PALAN, K., GREEN, A.N., ANDREWS, B., SINK, K. AND WILES, E.A., 2020. A morphometric analysis of the fluid flow features of the southern Orange Basin, South Africa. Marine Geology, 423, p.106145.

PAGANONI, M., KING, J.J., FOSCHI, M., MELLOR-JONES, K., CARTWRIGHT, J.A., 2019. A natural gas hydrate system on the Exmouth Plateau (NW shelf of Australia) sourced by thermogenic hydrocarbon leakage. Mar. Pet. Geol. 99, 370–392. https://doi.org/ 10.1016/j.marpetgeo.2018.10.029.

PRYER, L.L., ROMINE, K.K., LOUTIT, T.S., BARNES, R.G., 2002. Carnarvon Basin architecture and structure defined by the integration of mineral and petroleum exploration tools and techniques. The APPEA Journal 42(1), 287-309.

ROELOFSE, C, ALVES, T.M., GAFEIRA, J. 2020 Structural controls on shallow fluid flow and associated pockmark fields in the East Breaks area, northern Gulf of Mexico. Marine and Petroleum Geology. Vol. 112. ROHRMAN, M., 2013. Intrusive large igneous provinces below sedimentary basins: An example from the Exmouth Plateau (NW Australia). Journal of Geophysical Research: Solid Earth, Vol. 118.8, p. 4477-4487.

ROHEAD-O'BRIEN, H., ELDERS, C., 2018. Controls on Mesozoic rift-related uplift and syn- extensional sedimentation in the Exmouth Plateau. ASEG Ext. Abstr. 1

ROHRMAN, M. (2013). Intrusive large igneous provinces below sedimentary basins: An example from the Exmouth Plateau (NW Australia). Journal of Geophysical Research: Solid Earth,118(8), 4477-4487.

ROHRMAN, M. 2015. Delineating the Exmouth mantle plume (NW Australia) from denudation and magmatic addition estimates. Lithosphere, 7, 589–600, doi:10.1130/L445.1.

STAGG, H.M.J. and COLWELL, J.B. 1994. The structural foundations of the Northern Carnarvon Basin. In: PURCELL, G.P. and PURCELL, R.R. (eds) The Sedimentary Basins of Western Australia. Proceedings of Petroleum Exploration Society of Australia Symposium. Petroleum Exploration Society of Australia, Perth, Australia, 349–372.

STAGG, H.M.J., ALCOCK, M.B., BERNARDEL, G., MOORE, A.M.G., SYMONDS, P.A.andEXON, N.F. 2004. Geological Framework of the Outer Exmouth Plateau and Adjacent Ocean Basins. Geoscience Australia Record, 2004/13.

SVENSEN, H., PLANKE, S., MALTHE-SØRENSSEN, A., JAMTVEIT, B., MYKLEBUST, R., EIDEM, T. R., and REY, S. S. (2004). Release of methane from a volcanic basin as a mechanism for initial Eocene global warming. Nature, 429(6991), 542-545.

SVENSEN, H., JAMTVEIT, B., PLANKE, S., and CHEVALLIER, L. (2006). Structure and evolution of hydrothermal vent complexes in the Karoo Basin, South Africa. Journal of the Geological Society, 163(4), 671-682.

SWARBRICK, R.E., OSBORNE, M.J., AND YARDLEY, G.S., 2002. Comparison of overpressure magnitude resulting from the main generating mechanisms. In Huffman A. R., and Bowers G. L., (eds.), Pressure regimes in sedimentary basins and their prediction. AAPG Memoir, Vol. 76, p.1-12.

SWIFT M, BOYD R, O'BRIEN D. AND LORENZO J., 1992. Heat flow and thermal history of the Exmouth plateau. Proceedings of the Ocean Drilling Program, Scientific Results, Vol. 122.

TINGAY, M. R., HILLIS, R. R., SWARBRICK, R. E., MORLEY, C. K., and DAMIT, A. R. (2009). Origin of overpressure and pore-pressure prediction in the Baram province, Brunei. Aapg Bulletin, 93(1), 51-74.

TRAYNOR, J.J., SLADEN, C., 1997. Seepage in Vietnam – onshore and offshore examples. Mar. Pet. Geol. 14 (4), 345–362.

VAN TUYL, J., ALVES, T.M. AND CHERNS, L., 2018. Geometric and depositional responses of carbonate build-ups to Miocene sea level and regional tectonics offshore northwest Australia. Marine and Petroleum Geology, 94, pp.144-165.

VELAYATHAM, T., HOLFORD, S.P. AND BUNCH, M.A., 2018. Ancient fluid flow recorded by remarkably long, buried pockmark trains observed in 3D seismic data, Exmouth Plateau, Northern Carnarvon Basin. Marine and Petroleum Geology, 95, pp.303-313.

VELAYATHAM, T., HOLFORD, S.P., BUNCH, M., KING, R.C. and MAGEE, C. 3D Seismic Analysis of Ancient Subsurface Fluid Flow in the Exmouth Plateau, Offshore Western Australia, in KEEP, M. and MOSS, S.J. (Eds), The Sedimentary Basins of Western Australia V: Proceedings of the Petroleum Exploration Society of Australia Symposium, Perth, WA, 2019, 24 pp

WOODSIDE, 2011a. Alaric-1 (WA-434-P, Carnarvon Basin) Final well completion report. Woodside Energy Ltd.

WOODSIDE, 2011b. WA-434-P Claudius 3D Marine seismic survey interpretation report. Woodside Energy Ltd

ZHOU, F., FREDERICKS, L., LUFT, J., ORABY, M., JEFFRIES, M., PINDER, B., and KEOGH, S. (2020). A case study of mapping igneous sill distribution in coal measures using borehole and 3D seismic data. International Journal of Coal Geology, 103531.

Figure captions

Figure 1. Claudius 3D survey location and regional overview. *(a)* Regional framework of the Northern Carnarvon Basin, offshore Western Australia. Navy blue block represents the Claudius 3D survey in the Exmouth Plateau and the purple line indicates the location of the regional seismic section displayed in Fig. 1b. The top Triassic TR30.1_TS surface map is superimposed to bathymetric contours in blue and constrains the location of five wells used in this research. (b) Uninterpreted and (c) interpreted 2D regional seismic cross-section showing the key tectonostratigraphic sequences and structural architectures of the Exmouth Plateau. The Triassic and older strata is affected by domino-style extensional faults. Large igneous intrusions are present in this respective unit.

Figure 2. Seismo-chronostratigraphy chart of the Exmouth Plateau. Figure comprises simplified stratigraphy of the research area and tectonic events based on growth strata documented in the Claudius 3D survey and following Longley ***et al.***(2002). The sequence stratigraphy nomenclature folllows Exon ***et al.***(1992) and Marshall and Lang (2013).

Figure 3. Uninterpreted and interpreted seismic section highlighting details of the tectono-stratigraphic megasequences of the western Exmouth Plateau. Key interpreted horizons and their ages are also shown. The giant Mungaroo Formation is significantly affected by domino-style extensional faults with thin Late Jurassic to Early Cretaceous growth strata in their hangingwalls, suggesting fault activity during this time. Line location is shown in Figure 1a.

Figure 4. Characterisation of fluid escape pipes in the Claudius 3D survey. (a) Time structure map of the Upper Triassic Rhaetian (TR30.1_TS) surface showing the main NNE-and NNW-trending extensional faults of the research area. The study area is focused on the eastern part of the Claudius survey where most fluid escape pipes occur as shown by the yellow polygon. Additionally, several mounds located towards the west of the survey area characterise the Uppermost Triassic carbonate reef system in the Claudius 3D survey. (b) Detailed image showing the NNW-trending pockmark trains at the Rhaetian level. (c) Vertical seismic section illustrates details of a fluid escape pipe recorded measurements to analyse their morphology.

Table 1. Stratigraphic units and seismic horizons characteristics. Table summarises the three main regional tectonostratigraphic megasequences and their respective sequences identified from the Claudius 3D survey, displaying independent selected horizons, their age, and seismic polarity.

Figure 5. Spatial distribution of fluid escape pipes and main structures (a) TR30.1_TS surface map of the research area showing the three types of fluid escape pipes identified in this study; blowout pipes (blue), seepage (yellow) and hydrothermal (orange). Aligned clusters in blue represent the common distribution of fluid escape pipes. (b) Rose diagram displaying a strong spatial relationship between fluid escape pipes, and the minor intra-graben fault arrays with a dominant NNW direction. Note the NNE dominant trending of the half-graben bounding faults. and the half-graben-bounding fault array with a NNE direction. (c) Detail map of the Rhaetian showing the spatial distribution of clustered and isolated pipes within the minor array in the TR30.1 map surface.

Figure 6. *Statistical morphological results.* (a) Numerical proportion of blowout, seepage and hydrothermal pipes in the research area. (b) Variation of the calculated average pipe column diameter encountered in fluid escape pipes. (c) Variation of pipe top terminus depth where most pipes end between 3-3.2 TWT. Such depth correlates with the Jurassic J40.0 SB regional horizon. (d) Length of fluid escape pipes where pipes being <1500m long are classified as small, <3000m long are medium and >3000 are considered long. (e) The root zone variation analysis shows the pipe bottom depth and respective maximus for blowout, seepage and hydrothermal pipes.

Figure 7. Detailed seismic cross section displayed as (a) normal amplitude and (b) ESP coherency extraction (dark colour reflections represent low coherency and light colours high coherency) displaying fluid escape pipes (P1-P5) conduit bottom and root zone in different stratigraphic levels.

Figure 8. Uninterpreted and interpreted seismic sections displaying fluid escape pipes top conduit terminus in the same J40.0 SB stratigraphic level with no signs of reactivation of further propagation above this horizon.

Figure 9. Schematic evolution of the western Exmouth Plateau. Rapid sedimentation and hydrocarbon maturation occurred during the Late Triassic extending to the Early Jurassic. Late Jurassic syn-rift developed the half graben array and emplaced igneous intrusions leading to the triggering of fluid escape pipes.

Figure 10. Schematic 3D diagram showing the occurrence of the three types of fluid escape pipes identified in this study and how these are related to the structures. Note how the pipes are sourced from different stratigraphic levels and their trend is parallel to minor fault strike. Pipes may nucleate at or along the fault planes.

Figure 11. 2D models showing the evolution of fluid escape pipes in the western Exmouth Plateau. (a) Rapid sedimentation of the Mungaroo Formation and hydrocarbon generation induce overpressure; (b) Formation of NNE- and NNW-trending extensional faults during rift development together with sills emplacement induce excess of overpressure and fluid escape pipe formation; (c) During the main syn-rift, major faults propagation and linkages, release of overpressure and expulsion of the escape fluid at the Oxfordian level; (d) End of rifting and cessation of fault activity, burial of paleo-pockmarks by Early Cretaceous strata; (e) During passive margin stage, major extensional faults were reactivated together with the development of extensive polygonal faults.

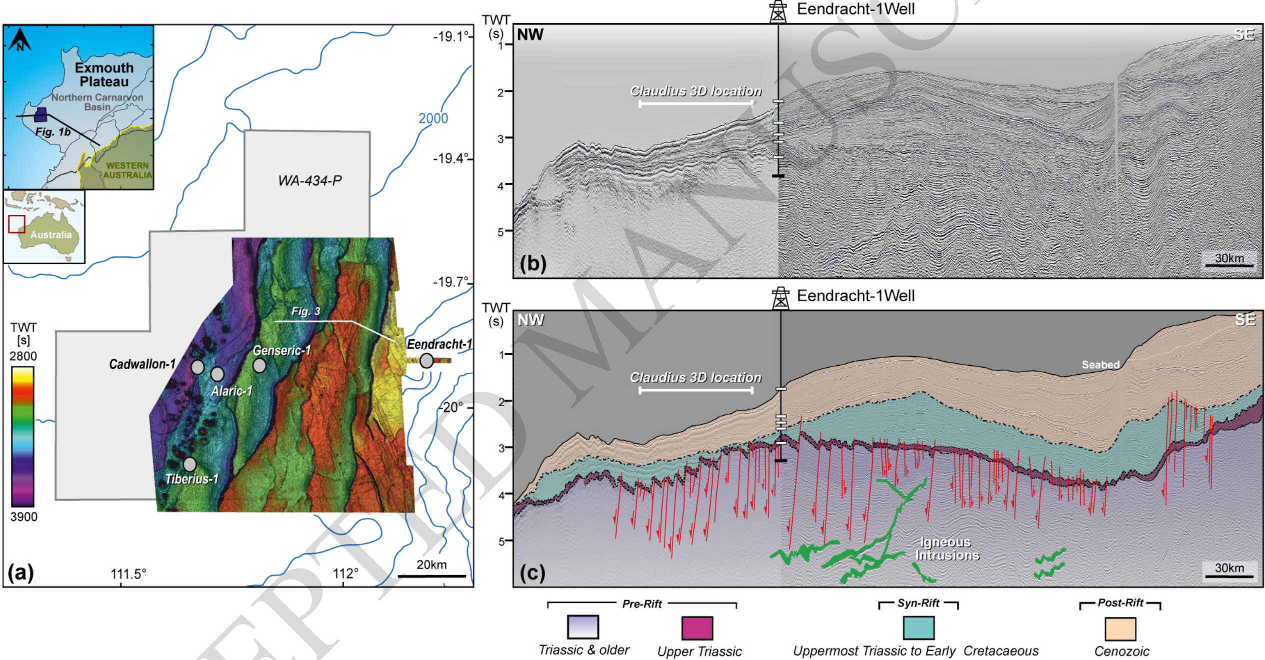
Exmouth Plateau
Northern Carnarvon Basin
Fig. 1b
WESTERN AUSTRALIA
Australia
N
WA-434-P
2000
-19.1°
-19.4°
-19.7°
-20°
Fig. 3
Eendracht-1
Genseric-1
Cadwallon-1
Alaric-1
Tiberius-1
TWT [s]
2800
3900
111.5°
112°
20km
(a)
Eendracht-1Well
TWT (s)
NW
SE
Claudius 3D location
1
2
3
4
5
30km
(b)
Eendracht-1Well
TWT (s)
NW
SE
Seabed
Claudius 3D location
Igneous Intrusions
30km
(c)
Pre-Rift
Syn-Rift
Post-Rift
Triassic & older
Upper Triassic
Uppermost Triassic to Early Cretacaeous
Cenozoic

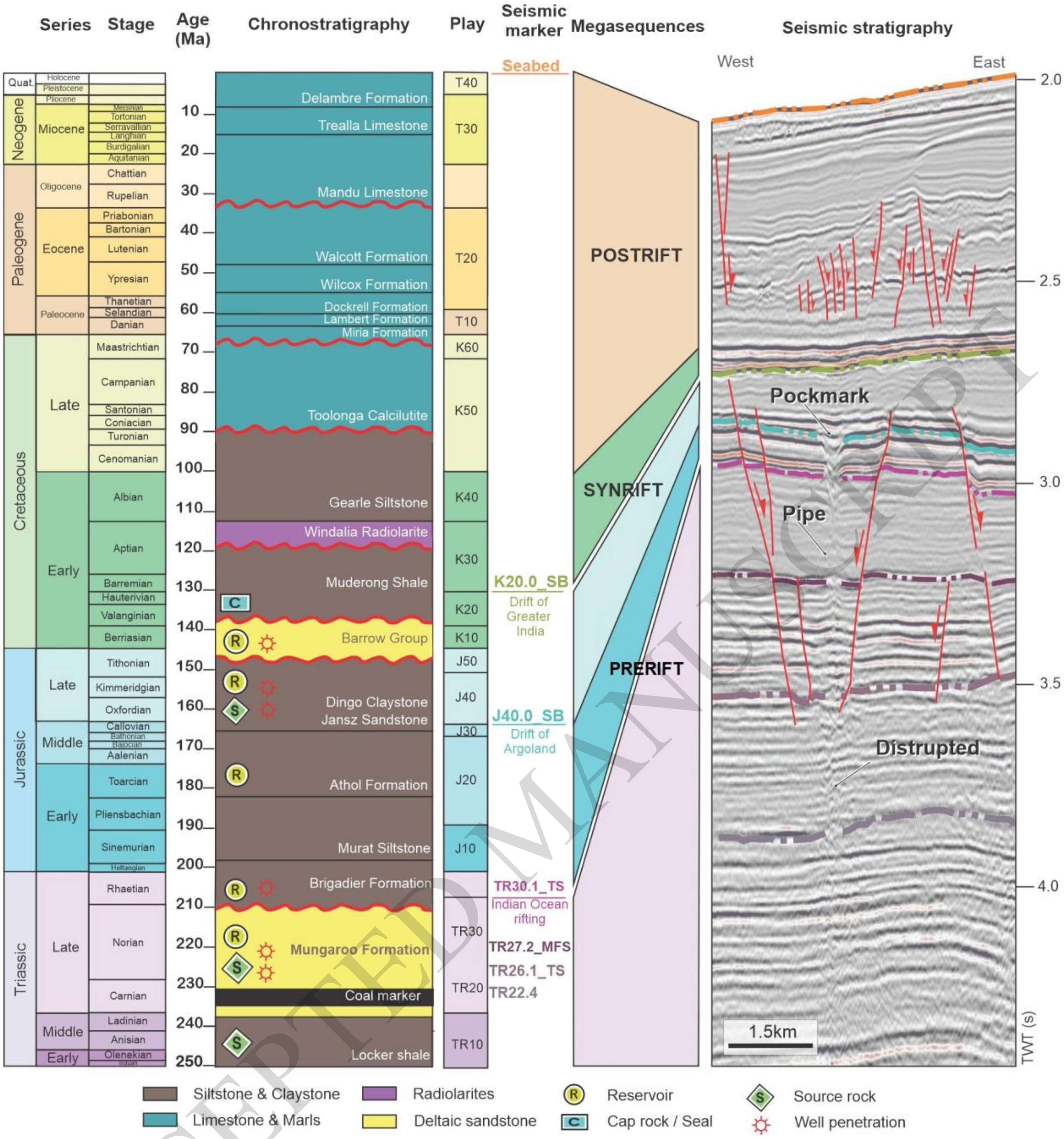

Series
Stage
Age (Ma)
Chronostratigraphy
Play
Seismic marker
Megasequences
Seismic stratigraphy
West
East
Seabed
Quat.
Neogene
Miocene
Paleogene
Oligocene
Eocene
Paleocene
Cretaceous
Late
Early
Jurassic
Middle
Triassic
Holocene
Pleistocene
Pliocene
Messinian
Tortonian
Serravallian
Langhian
Burdigalian
Aquitanian
Chattian
Rupelian
Priabonian
Bartonian
Lutenian
Ypresian
Thanetian
Selandian
Danian
Maastrichtian
Campanian
Santonian
Coniacian
Turonian
Cenomanian
Albian
Aptian
Barremian
Hauterivian
Valanginian
Berriasian
Tithonian
Kimmeridgian
Oxfordian
Callovian
Bathonian
Bajocian
Aalenian
Toarcian
Pliensbachian
Sinemurian
Hettangian
Rhaetian
Norian
Carnian
Ladinian
Anisian
Olenekian
10
20
30
40
50
60
70
80
90
100
110
120
130
140
150
160
170
180
190
200
210
220
230
240
250
Delambre Formation
Trealla Limestone
Mandu Limestone
Walcott Formation
Wilcox Formation
Dockrell Formation
Lambert Formation
Miria Formation
Toolonga Calcilutite
Gearle Siltstone
Windalia Radiolarite
Muderong Shale
Barrow Group
Dingo Claystone
Jansz Sandstone
Athol Formation
Murat Siltstone
Brigadier Formation
Mungaroo Formation
Coal marker
Locker shale
T40
T30
T20
T10
K60
K50
K40
K30
K20
K10
J50
J40
J30
J20
J10
TR30
TR20
TR10
K20.0_SB
Drift of Greater India
J40.0_SB
Drift of Argoland
TR30.1_TS
Indian Ocean rifting
TR27.2_MFS
TR26.1_TS
TR22.4
POSTRIFT
SYNRIFT
PRERIFT
Pockmark
Pipe
Distrupted
1.5km
2.0
2.5
3.0
3.5
4.0
TWT (s)
Siltstone & Claystone
Limestone & Marls
Radiolarites
Deltaic sandstone
Reservoir
Cap rock / Seal
Source rock
Well penetration

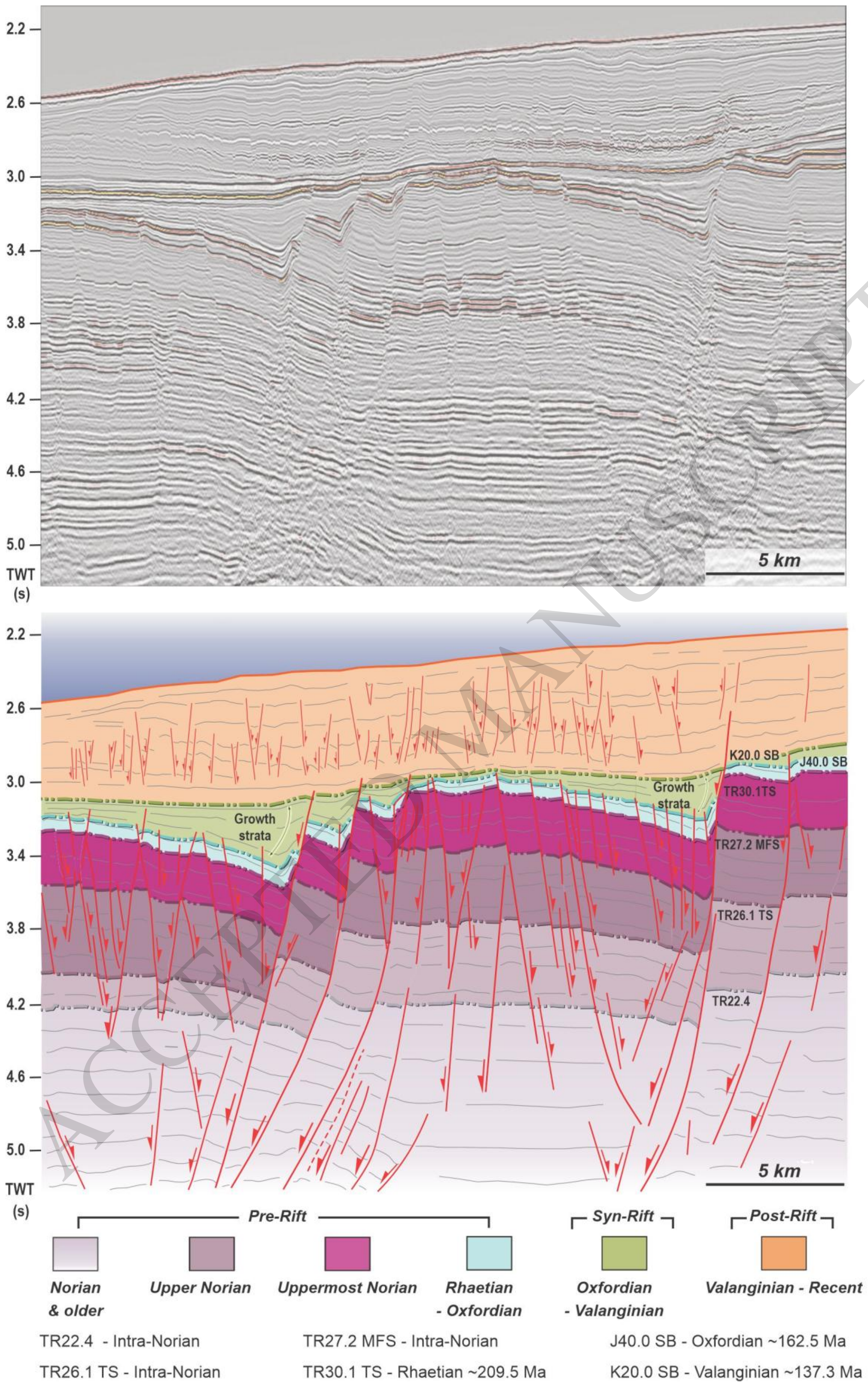
2.2
2.6
3.0
3.4
3.8
4.2
4.6
5.0
TWT (s)
5 km
Growth strata
Growth strata
K20.0 SB
J40.0 SB
TR30.1TS
TR27.2 MFS
TR26.1 TS
TR22.4
Pre-Rift
Syn-Rift
Post-Rift
Norian & older
Upper Norian
Uppermost Norian
Rhaetian - Oxfordian
Oxfordian - Valanginian
Valanginian - Recent
TR22.4 - Intra-Norian
TR26.1 TS - Intra-Norian
TR27.2 MFS - Intra-Norian
TR30.1 TS - Rhaetian ~209.5 Ma
J40.0 SB - Oxfordian ~162.5 Ma
K20.0 SB - Valanginian ~137.3 Ma

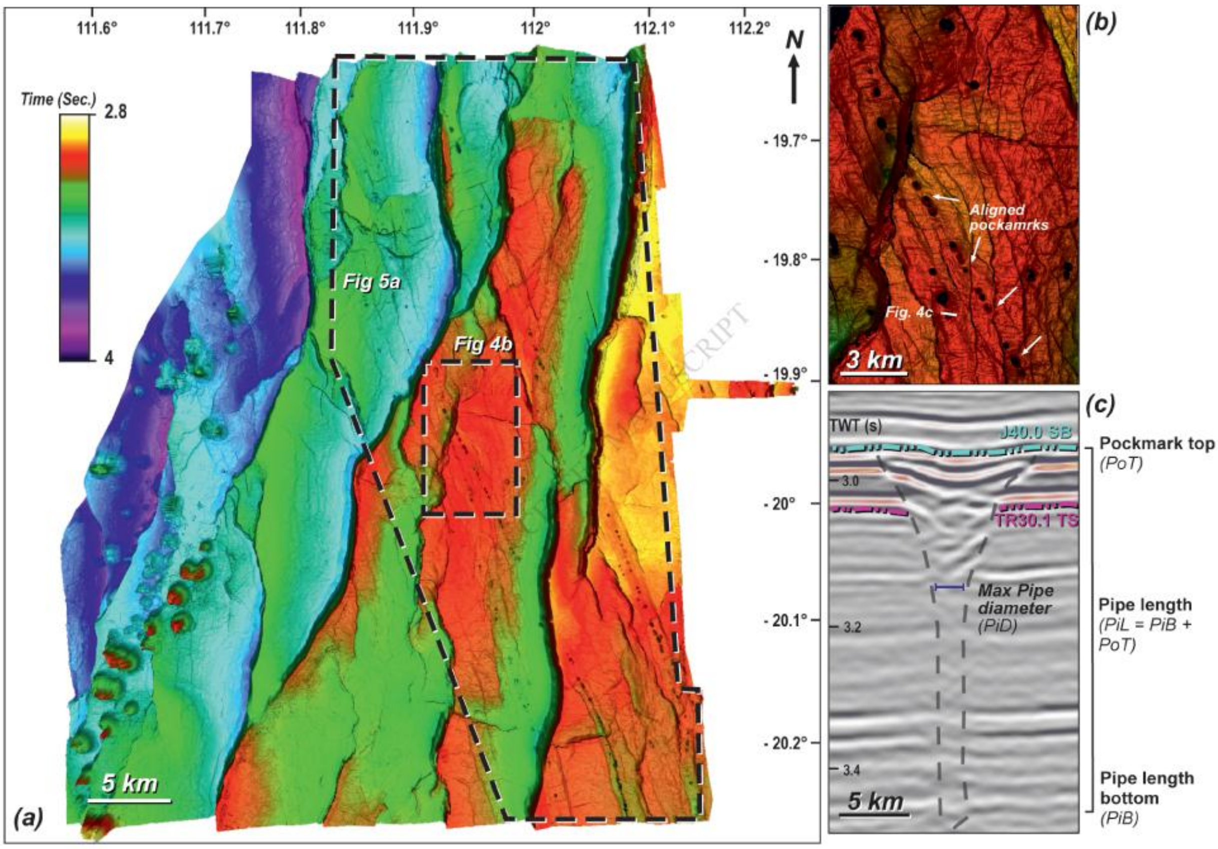

111.6°
111.7°
111.8°
111.9°
112°
112.1°
112.2°
N
Time (Sec.)
2.8
4
19.7°
19.8°
19.9°
20°
20.1°
20.2°
Fig 5a
Fig 4b
5 km
(a)
(b)
Aligned pockamrks
Fig. 4c
3 km
(c)
TWT (s)
J40.0 SB
3.0
TR30.1 TS
Max Pipe diameter (PiD)
3.2
3.4
5 km
Pockmark top (PoT)
Pipe length (PiL = PiB + PoT)
Pipe length bottom (PiB)

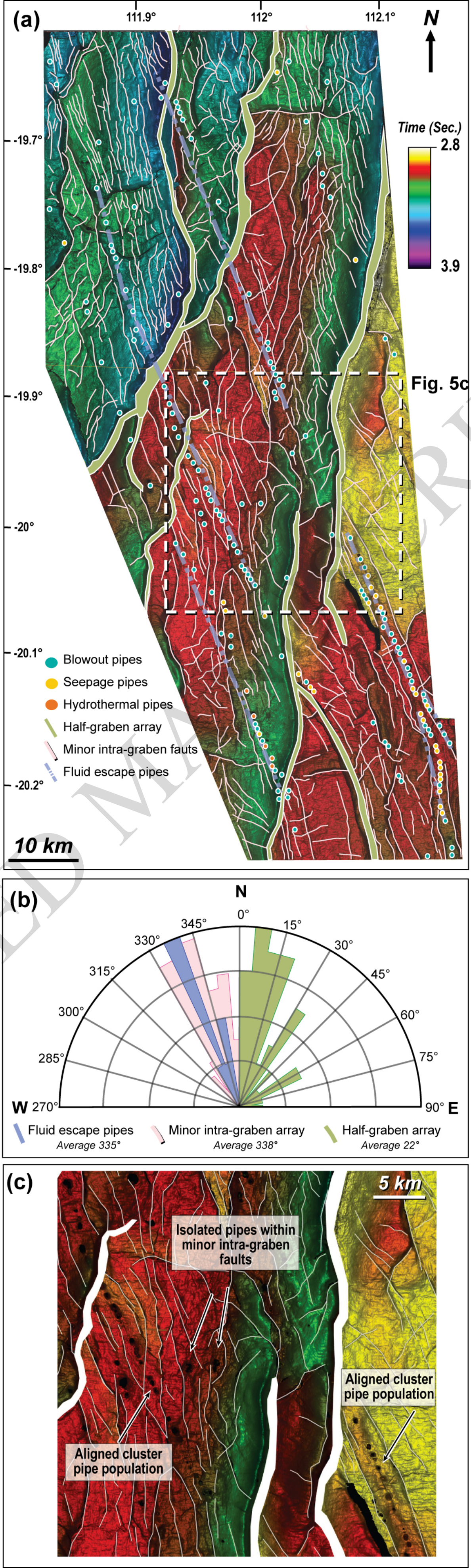
(a)
111.9°
112°
112.1°
N
Time (Sec.)
2.8
3.9
-19.7°
-19.8°
-19.9°
-20°
-20.1°
-20.2°
Fig. 5c
Blowout pipes
Seepage pipes
Hydrothermal pipes
Half-graben array
Minor intra-graben fauts
Fluid escape pipes
10 km
(b)
N
0°
15°
30°
45°
60°
75°
90° E
W 270°
285°
300°
315°
330°
345°
Fluid escape pipes
Average 335°
Minor intra-graben array
Average 338°
Half-graben array
Average 22°
(c)
5 km
Isolated pipes within minor intra-graben faults
Aligned cluster pipe population
Aligned cluster pipe population

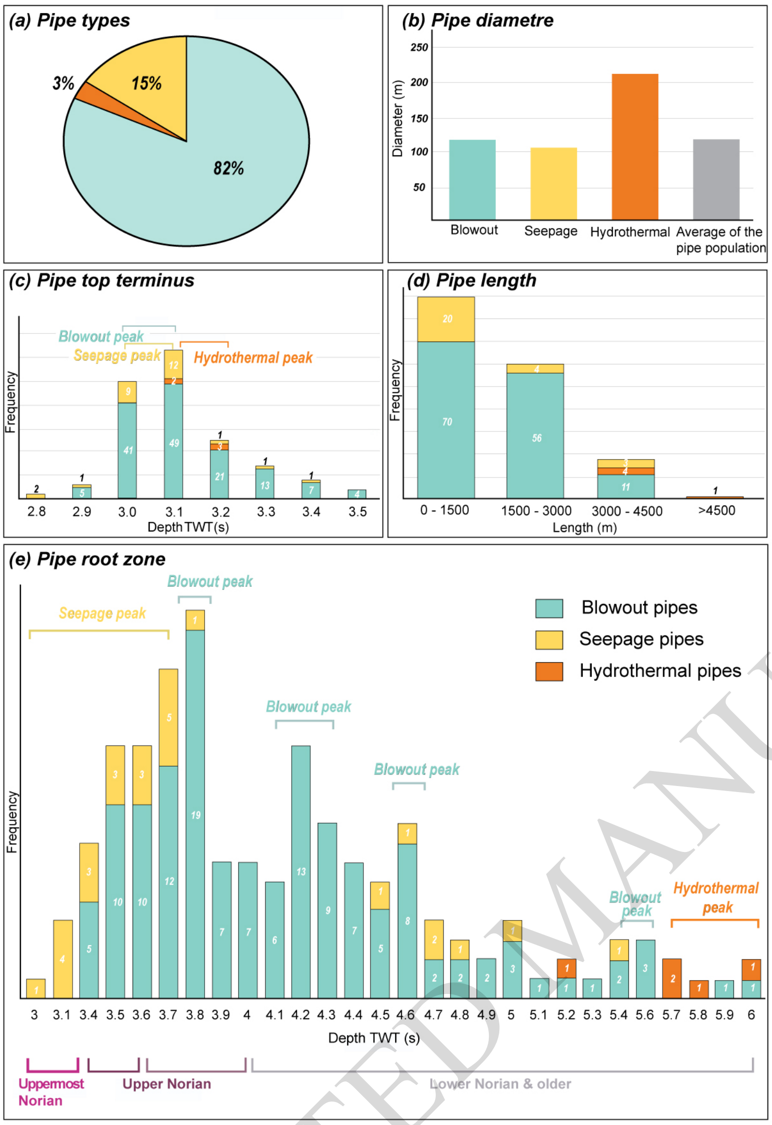

(a) Pipe types
3%
15%
82%
(b) Pipe diametre
Diameter (m)
250
200
150
100
50
Blowout
Seepage
Hydrothermal
Average of the pipe population
(c) Pipe top terminus
Blowout peak
Seepage peak
Hydrothermal peak
Frequency
2.8
2.9
3.0
3.1
3.2
3.3
3.4
3.5
Depth TWT(s)
(d) Pipe length
Frequency
0 - 1500
1500 - 3000
3000 - 4500
>4500
Length (m)
(e) Pipe root zone
Blowout peak
Seepage peak
Hydrothermal peak
Blowout pipes
Seepage pipes
Hydrothermal pipes
Frequency
Depth TWT (s)
Uppermost Norian
Upper Norian
Lower Norian & older

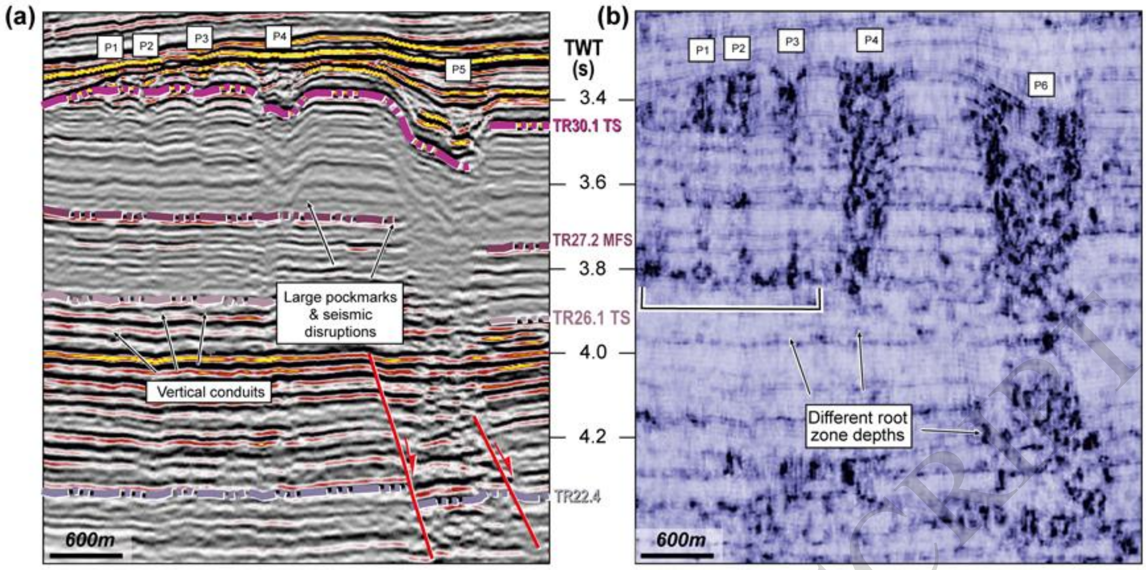
(a)
(b)
P1
P2
P3
P4
P5
P6
TWT (s)
3.4
3.6
3.8
4.0
4.2
TR30.1 TS
TR27.2 MFS
TR26.1 TS
TR22.4
Large pockmarks & seismic disruptions
Vertical conduits
Different root zone depths
600m
600m

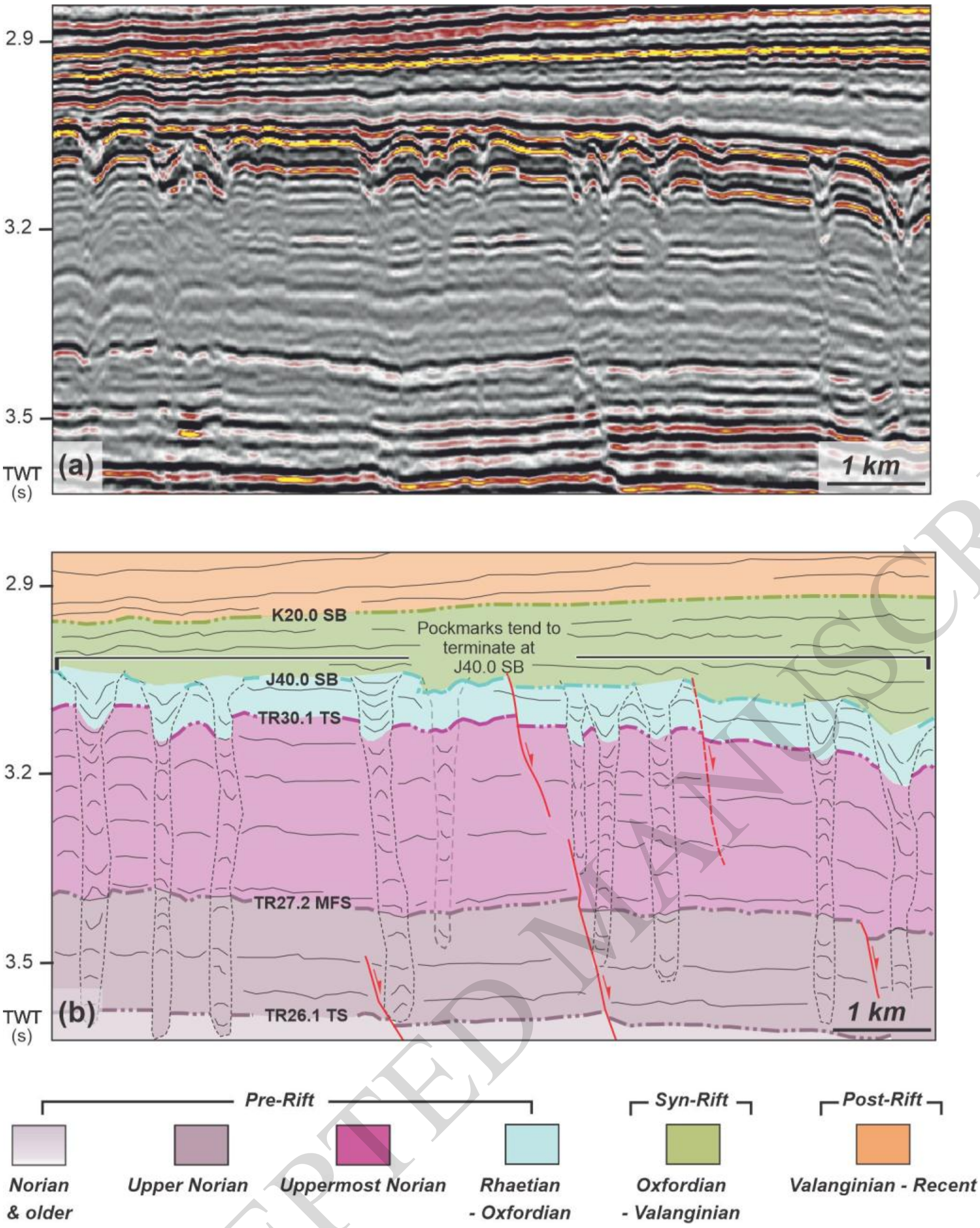
2.9
3.2
3.5
TWT
(s)
(a)
1 km
K20.0 SB
Pockmarks tend to terminate at J40.0 SB
J40.0 SB
TR30.1 TS
TR27.2 MFS
TR26.1 TS
(b)
Pre-Rift
Syn-Rift
Post-Rift
Norian & older
Upper Norian
Uppermost Norian
Rhaetian - Oxfordian
Oxfordian - Valanginian
Valanginian - Recent

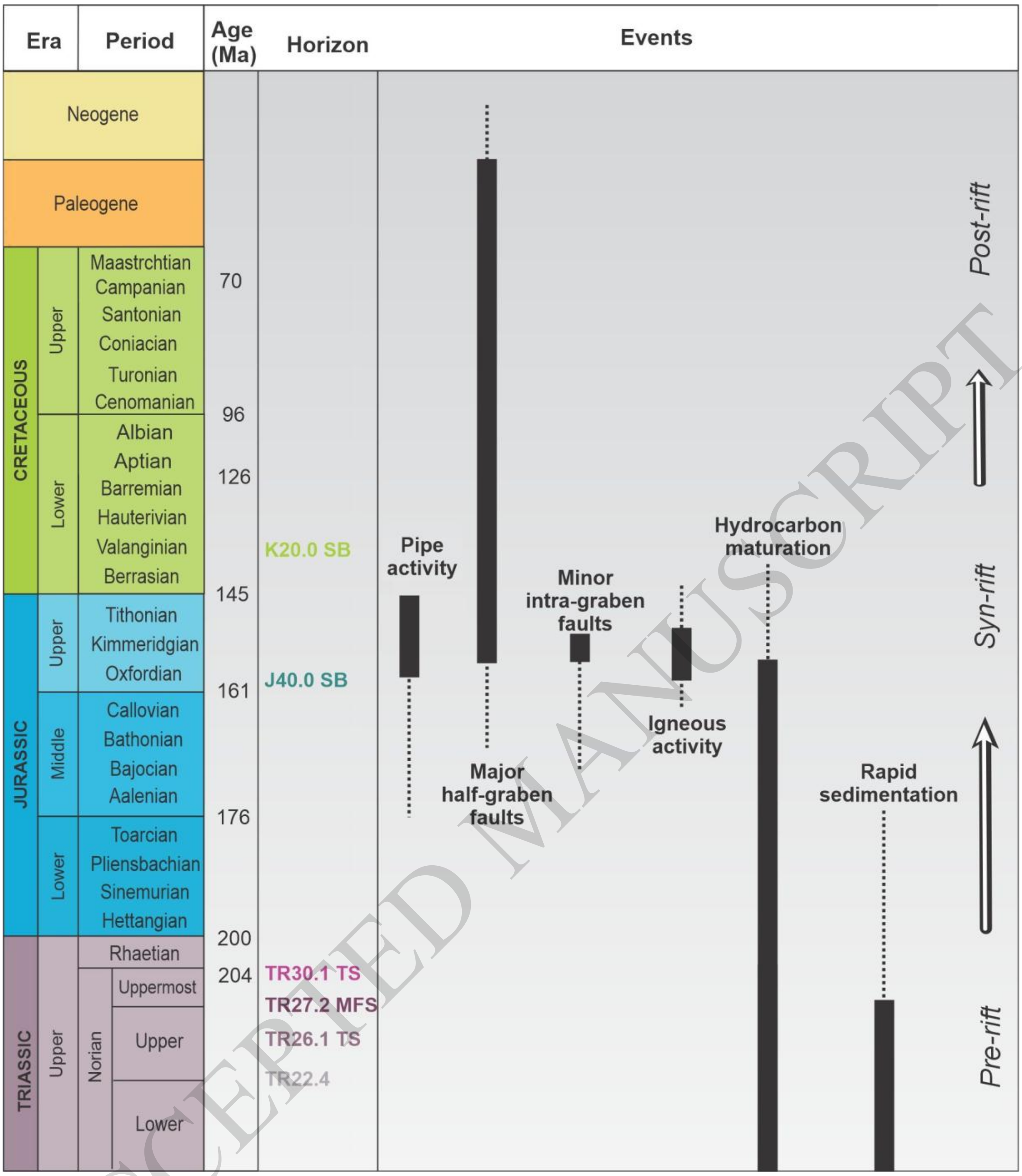
Era
Period
Age (Ma)
Horizon
Events
Neogene
Paleogene
CRETACEOUS
Upper
Lower
Maastrchtian
Campanian
Santonian
Coniacian
Turonian
Cenomanian
Albian
Aptian
Barremian
Hauterivian
Valanginian
Berrasian
JURASSIC
Upper
Middle
Lower
Tithonian
Kimmeridgian
Oxfordian
Callovian
Bathonian
Bajocian
Aalenian
Toarcian
Pliensbachian
Sinemurian
Hettangian
TRIASSIC
Upper
Norian
Rhaetian
Uppermost
Upper
Lower
70
96
126
145
161
176
200
204
K20.0 SB
J40.0 SB
TR30.1 TS
TR27.2 MFS
TR26.1 TS
TR22.4
Pipe activity
Major half-graben faults
Minor intra-graben faults
Igneous activity
Hydrocarbon maturation
Rapid sedimentation
Post-rift
Syn-rift
Pre-rift

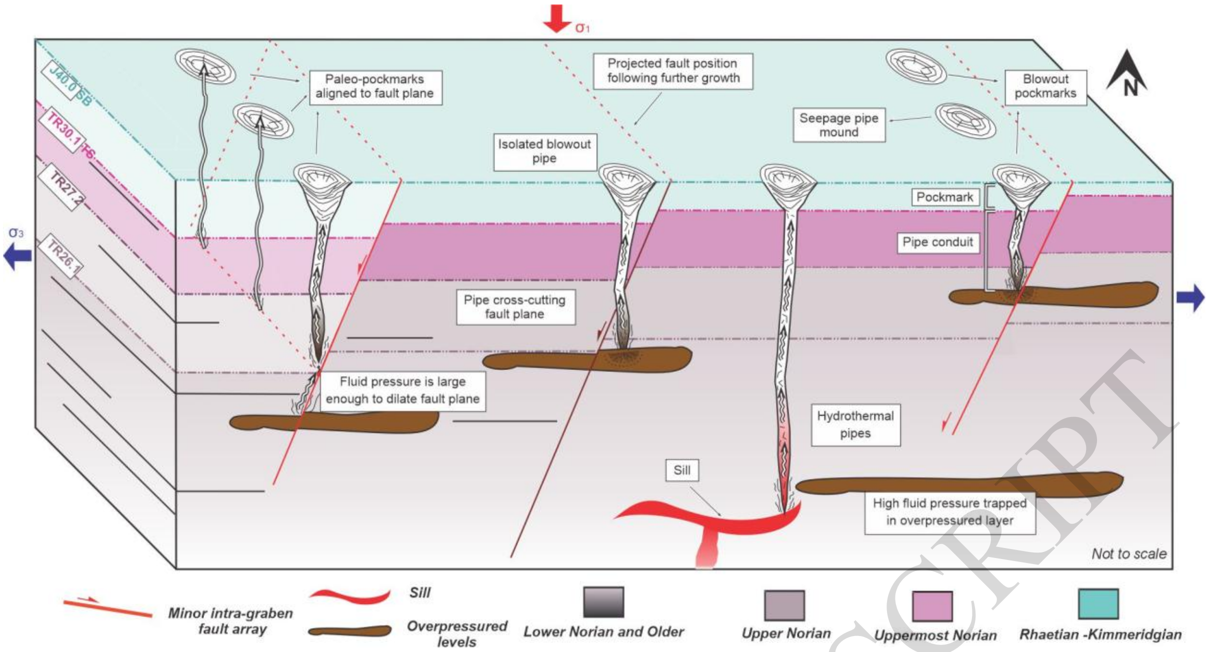
σ1
σ3
J40.0 SB
TR30.1 FS
TR27.2
TR26.1
Paleo-pockmarks aligned to fault plane
Projected fault position following further growth
Blowout pockmarks
N
Seepage pipe mound
Isolated blowout pipe
Pockmark
Pipe conduit
Pipe cross-cutting fault plane
Fluid pressure is large enough to dilate fault plane
Hydrothermal pipes
Sill
High fluid pressure trapped in overpressured layer
Not to scale
Minor intra-graben fault array
Sill
Overpressured levels
Lower Norian and Older
Upper Norian
Uppermost Norian
Rhaetian -Kimmeridgian

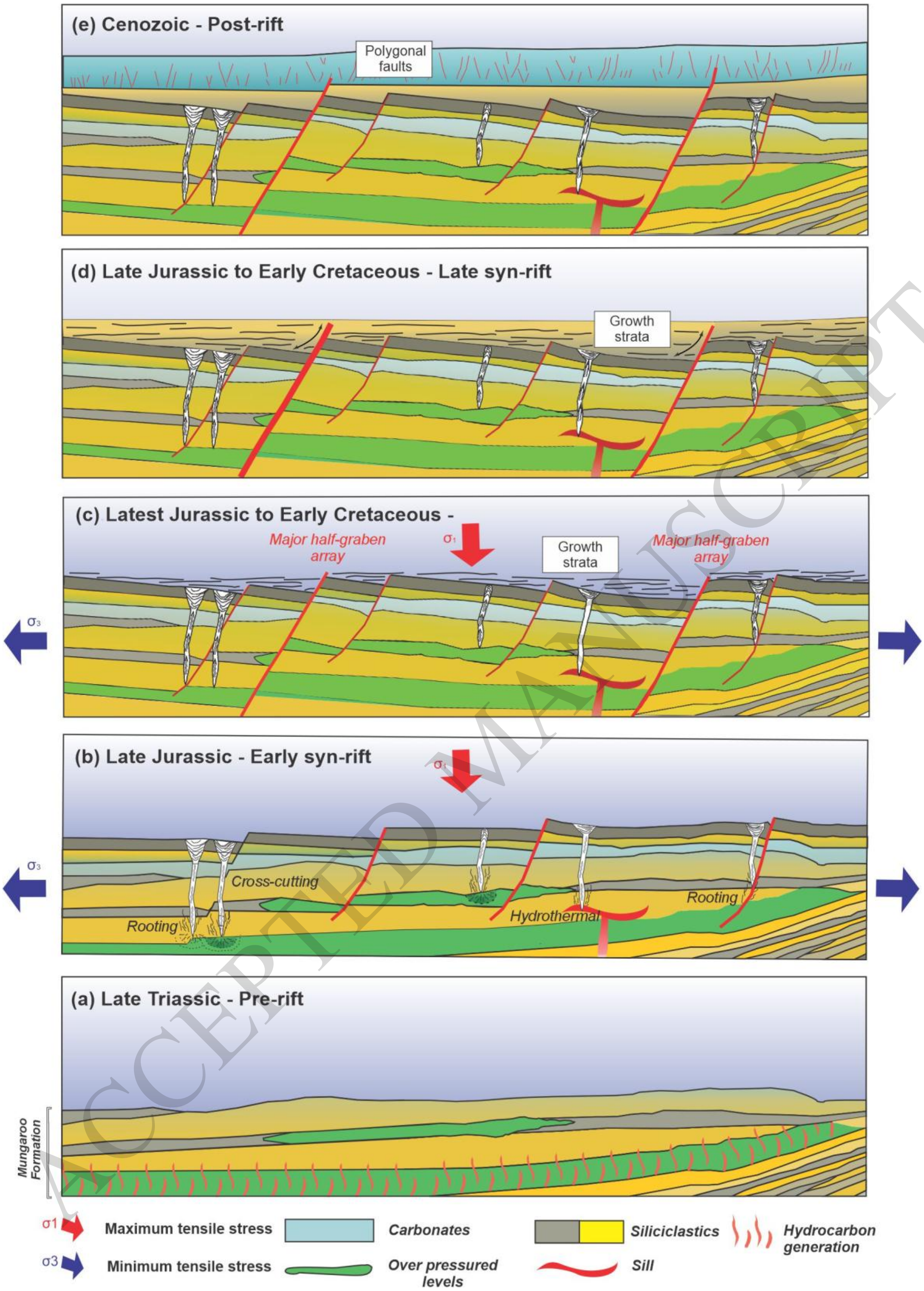

(e) Cenozoic - Post-rift
Polygonal faults
(d) Late Jurassic to Early Cretaceous - Late syn-rift
Growth strata
(c) Latest Jurassic to Early Cretaceous -
Major half-graben array
σ1
Growth strata
Major half-graben array
σ3
(b) Late Jurassic - Early syn-rift
σ1
σ3
Cross-cutting
Rooting
Hydrothermal
Rooting
(a) Late Triassic - Pre-rift
Mungaroo Formation
σ1 Maximum tensile stress
σ3 Minimum tensile stress
Carbonates
Over pressured levels
Siliciclastics
Sill
Hydrocarbon generation

Megasequence	*Chronostratigraphic unit*	*Top surface*	*Formation / Level*
Post-rift	*Valanginian to present day*	Seabed	Seabed
Synr-ift	*Oxfordian to Valanginian*	K20.0_SB	Barrow Group
Pre=r-ift	*Early Rhaetian to Oxfordian*	J40.0_SB	Intra Dingo Claystone
	Uppermost Norian to Early Rhaetian	TR30.1_TS	Top Mungaroo Formation
	Upper Norian	TR27.2_MFS	Intra Mungaroo Formation
		TR26.1_TS	
	Lower Norian	TR22.4	